SUPPORTING INFORMATION

Active Discovery of Donor:Acceptor Combinations For Efficient Organic Solar Cells

*Prateek Malhotra[a] , Juan C.Verduzco[b], Subhayan Biswas[a], Ganesh D. Sharma[a,c]**

[a]Department of Physics, The LNM Institute of Information Technology, Jamdoli, Jaipur 302031 (Rajasthan), India

[b]School of Materials Engineering and Birck Nanotechnology Center, Purdue University, West Lafayette, Indiana, 47907 USA

[c]Department of Electronics Engineering and communication, The LNM Institute of Information Technology, Jamdoli, Jaipur 302031(Rajasthan), India

*Corresponding author Email: Ganesh D. Sharma (gdsharma273@gmail.com and gdsharma@gmail.com)

Table S1 Dataset of 200 unique D:A combinations with corresponding PCE manually collected from the literature.

S. No.	Donor	Acceptor	J_{sc} (mA/cm^2)	V_{oc} (V)	FF	PCE (%)	Reference
1	D-0F	C8-ITIC	19.3	0.87	0.68	11.6	1
2	D-2F	C8-ITIC	18.8	0.94	0.69	12.2	1
3	D-4F	C8-ITIC	14.6	1.04	0.58	8.8	1
4	D-0F	ITIC	16.5	0.89	0.54	8	1
5	D-2F	ITIC	16.8	0.96	0.6	8.9	1
6	D-4F	ITIC	14.1	1.04	0.44	4.4	1
7	D-0F	IT-4F	16.4	0.77	0.62	7.8	1
8	D-2F	IT-4F	19.6	0.83	0.67	10.9	1
9	D-4F	IT-4F	18.4	0.93	0.62	9.9	1
10	PffBT4T-2DT	FBR	11.5	1.12	0.61	7.8	2
11	PffBT4T-2DT	IDTBR	15	1.05	0.62	9.95	2
12	PBDB-T	Y1	22.44	0.87	0.691	13.42	3
13	PBDB-T	Y2	23.56	0.82	0.694	13.4	3
14	P3TEA	SF-PDI2	13.27	1.11	0.643	9.5	4
15	PM6	Y11	24.3	0.897	0.63	13.8	5
16	PM6	IDST-4F	24.9	0.82	0.7	14.3	6
17	PM6	ID-4F	13.5	0.73	0.65	6.4	6

18	BDT-ffBX-DT	SFPDI	8.9	1.23	0.56	6.2	7
19	PM6	a-IT	16.6	0.907	0.762	11.46	8
20	PM6	N7IT	21.04	0.932	0.705	13.82	8
21	PM6	ITCPTC	17.6	0.95	0.734	12.3	9
22	PM6	ITC-2Cl	20.1	0.91	0.741	13.6	9
23	PM6	IT-4F	20	0.87	0.744	12.9	9
24	PM6	IT-4Cl	21.3	0.8	0.742	12.7	9
25	PTB7-Th	FOIC	22.5	0.74	0.703	11.7	10
26	PBDB-TF	BTP-4Cl (Y7)	25.4	0.867	0.75	16.5	11
27	PBDB-T	IT-4F	17.6	0.72	0.737	9.3	12
28	PBDBTz-2	IT-4F	17.9	0.86	0.675	10.4	12
29	PBDBTz-5	IT-4F	16.4	0.93	0.624	9.6	12
30	J52	ITCCM-O	9.23	1.34	0.442	5.5	13
31	PM6	Y6	25.5	0.825	0.72	15	14
32	J52	BTA3	14.62	1.07	0.6034	9.41	15
33	J52-Cl	BTA3	13.16	1.24	0.6662	10.5	15
34	PDCBT-2F	IT-M	10.3	1.13	0.55	6.4	16
35	PTB7-Th	IEICO	13.3	0.9	0.6	7.2	16
36	PBQ-QF	IEICO-4F	22.4	0.74	0.64	10.5	16
37	PvBDTTAZ	O-IDTBR	16.2	1.08	0.65	11.4	16
38	PBDB-T	NCBDT	18.64	0.847	0.646	10.19	17
39	PTPD3T	ITIC	13.5	0.91	0.68	8.4	18
40	PTPD2T	ITIC	12.3	0.96	0.6	7	18
41	PTPDBDT	ITIC	8.5	1.05	0.6	5.4	18
42	PBDB-T	BT-IC4F	21.4	0.69	0.664	9.83	19
43	PBDB-T	BT2F-IC4F	19.43	0.67	0.647	8.45	19
44	PBDB-T	BTOR-IC4F	20.57	0.8	0.696	11.48	19
45	PTB7-Th	IOTIC	10.7	0.88	0.6	6	20
46	PTB7-Th	IOTIC-2F	14.8	0.79	0.6	7.2	20
47	PTB7-Th	IOTIC-4F	20.5	0.72	0.68	10.2	20
48	PBDB-TF	BTP-eC7	24.1	0.843	0.735	14.9	21
49	PBDB-TF	BTP-eC9	26.2	0.839	0.811	17.8	21
50	PBDB-TF	BTP-eC11	25.7	0.851	0.775	16.9	21
51	PBDB-T	ITIC	14.09	0.892	0.7239	9.1	22
52	PBDB-T	IEICO-4F	16.32	0.754	0.615	7.59	22
53	PBT1-C	BTA3	10.89	1.21	0.565	8.1	23
54	PBDB-T	BTA3	9.96	1.16	0.598	7	23
55	PffBT2T-TT	O-IDTBR	14.73	1.08	0.64	10.1	24
56	J71	ZITI-S	17.39	0.811	0.6462	9.12	25
57	J71	ZITI-C	21.3	0.851	0.7276	13.18	25
58	J71	ZITI-N	21.78	0.876	0.72	13.68	25
59	PBDB-TF	AQx-1	22.18	0.89	0.6714	13.31	26
60	PBDB-TF	Aqx-2	25.38	0.86	0.7625	16.64	26
61	J61	BTA3	10.84	1.15	0.6714	8.25	27
62	PM6	3TP3T-4F	20.3	0.92	0.739	13.7	28
63	PM6	3TP3T-IC	13	1.05	0.65	8.9	28
64	PBDB-T	DOC6-IC	19.21	0.91	0.6011	10.52	29
65	PBDB-T	DOC8-IC	17.74	0.92	0.5765	9.41	29
66	PBDB-T	DOC2C6-IC	18.85	0.93	0.6333	11.1	29
67	PBDB-T	DOC2C6-2F	21.35	0.85	0.7315	13.24	29
68	PBDBT-2Cl	IT-4F	20.85	0.88	0.7718	14.16	30
69	PBDBT-2Cl	IT-2Cl	19.85	0.91	0.7574	13.68	30
70	PBDBT-2Cl	ITIC	14.86	1.02	0.6376	9.66	30

71	PBDBT-2Cl	IT-M	14.6	1.04	0.6046	9.18	[30]
72	PTB7-Th	ITIC	12.57	0.812	0.483	4.93	[31]
73	PTB7-Th	IT-M	13.89	0.846	0.557	6.55	[31]
74	PTB7-Th	IT-DM	13.82	0.892	0.546	6.71	[31]
75	PTB7-Th	IDT-2BR	11.54	1.056	0.511	6.19	[31]
76	PE71	Y6	22.49	0.82	0.66	12.03	[32]
77	PE72	Y6	18.98	0.83	0.62	9.74	[32]
78	PM6	Y18	23.86	0.87	0.636	13.32	[33]
79	PBT1-C	IDTT-C6-TIC	17	0.85	0.667	9.6	[34]
80	PBT1-C	IDTT-C8-TIC	20.3	0.88	0.746	13.4	[34]
81	PBT1-C	IDTT-C10-TIC	18.1	0.98	0.713	12.5	[34]
82	PBDB-TF	BTP-0F	15.2	0.96	0.565	8.2	[35]
83	PBDB-TF	BTP-2F	22.1	0.89	0.717	14.1	[35]
84	PBDB-TF	BTP-6F	25.9	0.81	0.728	15.3	[35]
85	PTH37	i-IEICO-4F	17.7	0.95	0.572	9.64	[36]
86	PMT49	i-IEICO-4F	17.6	0.98	0.574	9.82	[36]
87	PMOT39	i-IEICO-4F	15.4	1.01	0.508	7.9	[36]
88	PMTT56	i-IEICO-4F	14.1	1.05	0.508	7.57	[36]
89	PTH37	i-IEICO-2F	15	0.99	0.55	8.16	[36]
90	PMT49	i-IEICO-2F	15.6	1.01	0.539	8.49	[36]
91	PMOT39	i-IEICO-2F	10.6	1.05	0.539	6	[36]
92	PMTT56	i-IEICO-2F	7.9	1.07	0.486	4.1	[36]
93	PTH37	i-IEICO	9	1.02	0.486	4.46	[36]
94	PMT49	i-IEICO	8.6	1.05	0.455	4.11	[36]
95	PTB7-Th	i-IEICO-4F	16.5	0.83	0.563	7.76	[36]
96	J52	i-IEICO-4F	19.5	0.87	0.6	10.18	[36]
97	J61	i-IEICO-4F	17.6	0.94	0.568	9.4	[36]
98	J71	i-IEICO-4F	16.6	0.97	0.541	8.72	[36]
99	PTB7-Th	IEICO-4F	22.9	0.72	0.562	9.27	[36]
100	J52	IEICO-4F	21.8	0.73	0.484	7.72	[36]
101	J61	IEICO-4F	16.2	0.75	0.489	5.94	[36]
102	PMT49	IEICO-4F	12.5	0.85	0.422	4.5	[36]
103	J52	FOIC	24.9	0.66	0.519	8.53	[36]
104	J71	FOIC	20.3	0.77	0.54	8.48	[36]
105	PBDB-T	FOIC	21.2	0.69	0.444	6.53	[36]
106	PBDB-T-2Cl	FOIC	12.7	0.83	0.543	5.75	[36]
107	PMT49	FOIC	20.7	0.82	0.536	9.11	[36]
108	PMTT56	FOIC	14.3	0.87	0.568	7.08	[36]
109	PMT49	Y6	26	0.81	0.512	10.81	[36]
110	PMOT39	Y6	22.1	0.82	0.493	8.97	[36]
111	PMTT56	Y6	26.4	0.86	0.509	11.59	[36]
112	PM7	Y6	24.89	0.879	0.691	15.12	[37]
113	DR3TBDTT	O-IDTBR	8.47	1.14	0.425	4.12	[38]
114	BTTzR	Y6	23.2	0.88	0.68	13.9	[39]
115	PBDTSi-TZ	IT-4F	19.52	0.781	0.7381	11.26	[40]
116	PBDTCl-TZ	IT-4F	20.4	0.837	0.7152	12.21	[40]
117	PFBCPZ	IT-4F	21.2	0.92	0.785	15.3	[41]
118	PTQ7	Y6	18.65	0.71	0.434	5.75	[42]
119	PTQ9	Y6	23.72	0.82	0.54	10.5	[42]
120	PTQ10	Y6	24.81	0.87	0.751	16.21	[42]
121	L68	TT-PT-T-4F	21.25	0.85	0.701	12.72	[43]
122	L2	TT-PT-T-4F	22.17	0.86	0.736	14	[43]

123	PM6	BP4T-4F	26.3	0.839	0.777	17.1	44
124	PM6	BP5T-4F	24.6	0.888	0.763	16.7	44
125	PM6	ABP4T-4F	22	0.922	0.751	15.2	44
126	PBDB-TF	F-2Cl	19.97	0.875	0.737	12.87	45
127	PBDB-TF	3TT-OCIC	24.4	0.785	0.65	12.43	45
128	C1	IT-4F	13.91	0.98	0.61	8.31	46
129	J52-F	BTA13	11.55	1.18	0.6134	8.36	47
130	J71	IDTT-BH	17.77	0.9	0.691	11.05	48
131	J71	IDTT-OBH	14.75	0.92	0.61	8.02	48
132	PDCBT	IDTT-BH	17.15	0.88	0.686	10.35	48
133	PDCBT	IDTT-OBH	13.97	0.91	0.648	8.24	48
134	PBDB-T	IDTT-BH	16.86	0.85	0.692	9.92	48
135	PBDB-T	IDTT-OBH	17.46	0.87	0.72	10.93	48
136	J52	ITIC	13.11	0.73	0.578	5.51	49
137	J60	ITIC	16.33	0.91	0.6038	8.97	49
138	J61	ITIC	17.43	0.89	0.6148	9.53	49
139	J62	ITIC	16.85	0.915	0.7009	10.81	50
140	J63	ITIC	15.72	0.868	0.5958	8.13	50
141	J64	ITIC	15.4	0.889	0.6271	8.59	50
142	PBQ-0F	ITIC	16.16	0.69	0.5991	6.68	51
143	PBQ-QF	ITIC	17.16	0.83	0.6249	8.9	51
144	PBQ-4F	ITIC	17.87	0.95	0.668	11.34	51
145	J71	m-MeIC	18.45	0.919	0.692	11.73	52
146	PBDB-T	m-MeIC	18.16	0.843	0.697	10.68	52
147	PCE-10	m-MeIC	16.52	0.796	0.617	8.12	52
148	PTPDBDT	H-ITIC	9.1	1.04	0.59	5.6	53
149	PTPDBDT	F-ITIC	14.1	0.94	0.66	8.8	53
150	PTPDBDT	Cl-ITIC	15.6	0.94	0.65	9.5	53
151	PTPDBDT	Br-ITIC	15.4	0.93	0.66	9.4	53
152	PTPDBDT	I-ITIC	14.5	0.95	0.65	8.9	53
153	FTAZ	INIC	13.51	0.957	0.579	7.7	54
154	FTAZ	INIC1	16.63	0.929	0.643	10.1	54
155	FTAZ	INIC2	17.56	0.903	0.668	10.8	54
156	FTAZ	INIC3	19.44	0.857	0.674	11.5	54
157	PBDB-T	IEIC	15.05	1.02	0.48	7.3	55
158	PBDB-TF	IE-4F	18.23	0.91	0.56	9.3	55
159	PBDB-T	IE-4F	21.35	0.87	0.58	10.8	55
160	PBDB-TF	IE-4CL	17.82	0.89	0.61	9.7	55
161	PBDB-T	IE-4CL	21.49	0.86	0.6	11.1	55
162	PBFB-T-SF	IT-4F	20.5	0.88	0.719	12.97	56
163	PTB7-Th	SCPDT-PDI4	14.6	0.84	0.577	7.11	57
164	PffBT-T3	TPPz-PDI4	12.5	0.987	0.56	6.9	58
165	PffBT-T3	TPE-PDI4	10.6	1.029	0.54	5.9	58
166	PTh37	ITIC	17.63	0.927	0.667	10.9	59
167	PMT49	ITIC	18.52	0.97	0.674	12.1	59
168	PET52	ITIC	15.74	0.976	0.642	9.94	59
169	PHT53	ITIC	13.69	1.01	0.574	8.05	59
170	P1	ITIC-m	15.51	0.97	0.64	9.62	60
171	P2	ITIC-m	17.64	1.04	0.7	12.84	60
172	PM6	L8-BO	25.72	0.87	0.815	18.32	61
173	PBDTT-DPP	IEICO-4F	18.5	0.679	0.648	8.14	62
174	D18	Y6	27.7	0.859	0.766	18.22	63
175	PBDB-T-SF	IT-4F	20.2	0.9	0.72	13.1	64
176	PTQ10	IDTCN	13.9	0.98	0.54	7.4	65

177	PTQ10	IDTPC	17.5	0.93	0.746	12.2	[65]
178	J51	ITIC	14.08	0.84	0.61	7.03	[66]
179	J50	ITIC	12.93	0.71	0.53	4.8	[66]
180	PTB7-Th	DICTF	15.23	0.86	0.5	6.54	[67]
181	PBDB-T	DICTF	10.3	0.93	0.59	5.65	[68]
182	PBDB-T	FDICTF	15.81	0.94	0.66	9.81	[68]
183	PBDB-T	NFBDT	16.97	0.872	0.608	8.99	[69]
184	PBDB-T	FDNCTF	16.3	0.93	0.72	11.2	[70]
185	PTB7-Th	IDT-N	13.02	0.73	0.577	5.5	[71]
186	PBDB-T	IDT-N	14.89	0.78	0.5912	6.9	[71]
187	PBDB-T	IDT-T-N	12.97	0.92	0.4479	5.4	[71]
188	PTB7-Th	IDIC	10.9	0.806	0.561	5.24	[72]
189	PDCBT	IDIC	11.31	0.814	0.641	6.28	[72]
190	J51	IDIC	12.24	0.796	0.66	6.94	[72]
191	PDBT-T1	IDIC	15.85	0.85	0.68	9.2	[72]
192	PTFBDT-BZS	IDIC	14.52	0.921	0.602	8.06	[72]
193	J70	m-ITIC	18.09	0.92	0.6982	11.62	[73]
194	J71	m-ITIC	18.09	0.944	0.7059	12.05	[73]
195	J72	m-ITIC	16.35	0.962	0.6503	10.23	[73]
196	J73	m-ITIC	16.45	0.974	0.6687	10.71	[73]
197	J74	m-ITIC	15.89	0.99	0.6118	9.63	[73]
198	J81	ITIC	13.96	0.94	0.6116	8.03	[74]
199	J81	m-ITIC	14.62	0.95	0.519	7.21	[74]
200	PM6	DTC-4F	20.2	0.94	0.7042	13.37	[75]

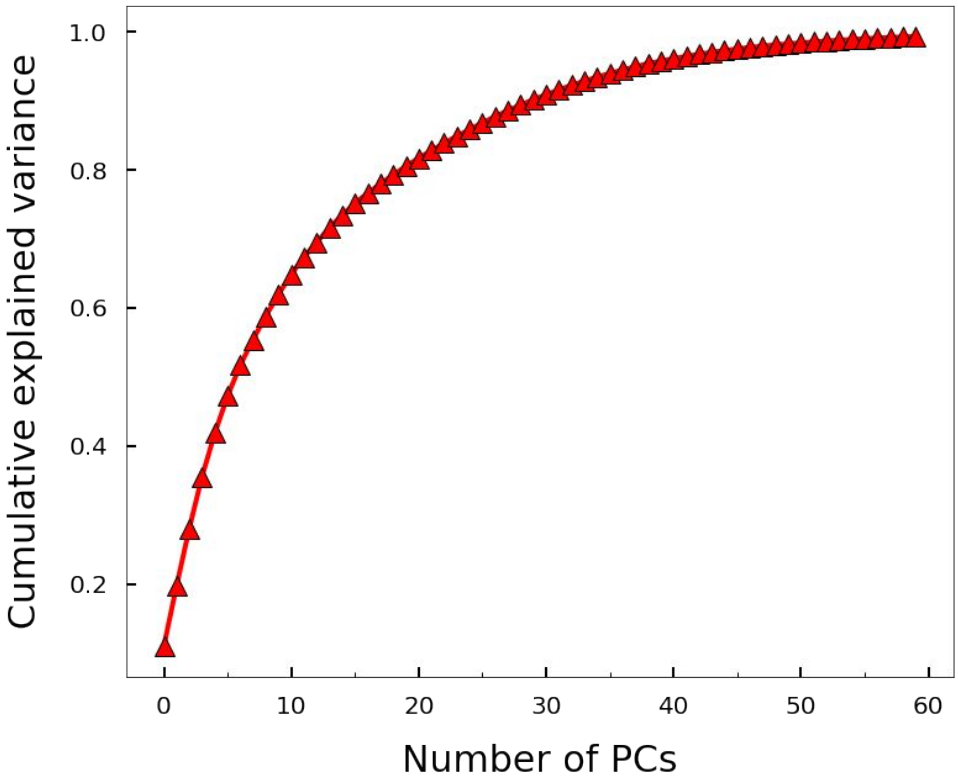

Figure S1 PCA analysis represents complete explanation of variance with 60 principal components.

Table S2 Randomly selected 10 D:A combinations with PCE less than 10%.

Index No.	Donor	Donor_structure	Acceptor	Acceptor_structure	PCE (%)
163	PffBT-T3	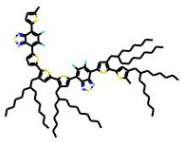	TPPz-PDI4	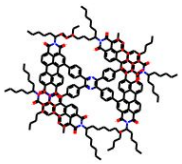	6.90
9	PffBT4T-2DT	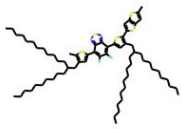	FBR	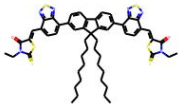	7.80
10	PffBT4T-2DT	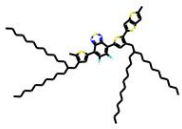	IDTBR	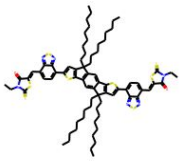	9.95

Index No.	Donor	Donor_structure	Acceptor	Acceptor_structure	PCE (%)
13	P3TEA	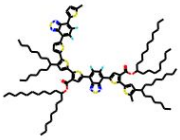	SF-PDI2	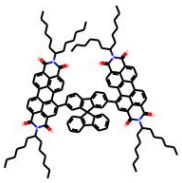	9.50
17	BDT-ffBX-DT		SFPDI	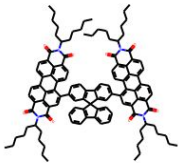	6.20
148	PTPDBDT	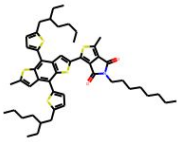	F-ITIC	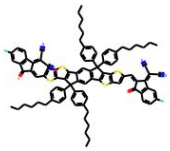	8.80
149	PTPDBDT	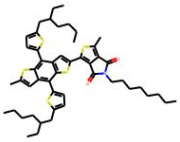	Cl-ITIC	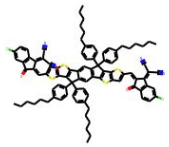	9.50
90	PMOT39	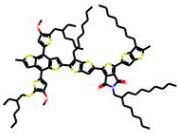	i-IEICO-2F	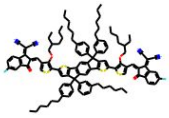	6.00
190	PDBT-T1	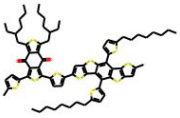	IDIC	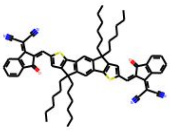	9.20
191	PTFBDT-BZS	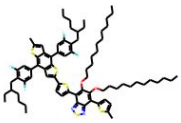	IDIC	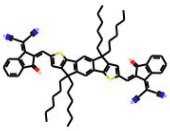	8.06

Table S3 D:A combination selected by MM acquisition function with corresponding test order. Best candidate is discovered in 40 iterations, and 15% PCE is crossed in 18 iterations.

Index No.	Donor	Donor_structure	Acceptor	Acceptor_structure	PCE (%)	Test order
150	PTPDBDT	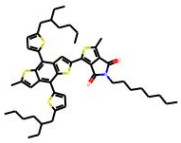	Br-ITIC	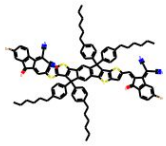	9.40	1
151	PTPDBDT	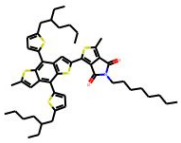	I-ITIC	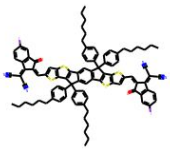	8.90	2
54	PffBT2T-TT	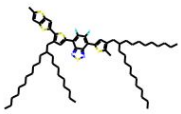	O-IDTBR	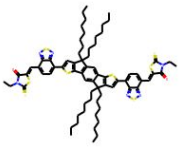	10.10	3
74	PTB7-Th	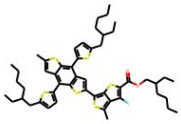	IDT-2BR	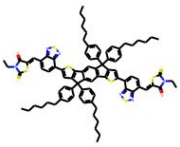	6.19	4
147	PTPDBDT		H-ITIC	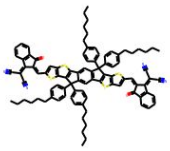	5.60	5
36	PvBDTTAZ	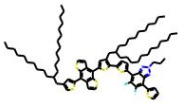	O-IDTBR	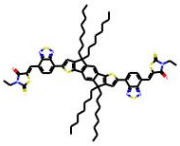	11.40	6
112	DR3TBDTT	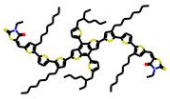	O-IDTBR	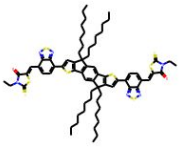	4.12	7
153	FTAZ	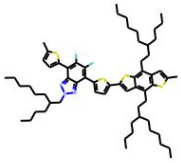	INIC1	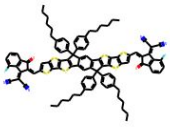	10.10	8

Index No.	Donor	Donor_structure	Acceptor	Acceptor_structure	PCE (%)	Test order
155	FTAZ	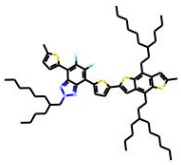	INIC3	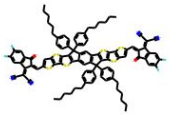	11.50	9
120	L68		TT-PT-T-4F	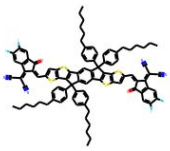	12.72	10
100	J61	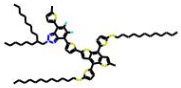	IEICO-4F	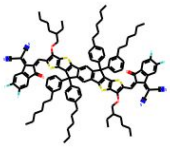	5.94	11
121	L2		TT-PT-T-4F	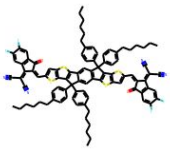	14.00	12
8	D-4F	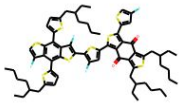	IT-4F	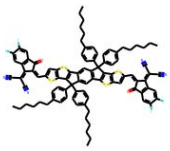	9.90	13
57	J71	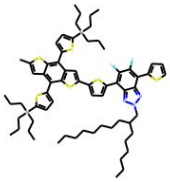	ZITI-N	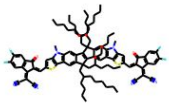	13.68	14
55	J71	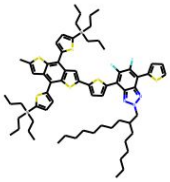	ZITI-S	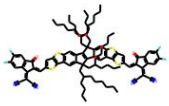	9.12	15
97	J71	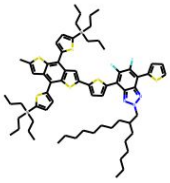	i-IEICO-4F	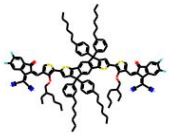	8.72	16
67	PBDBT-2Cl	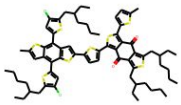	IT-4F	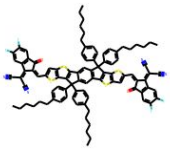	14.16	17

Index No.	Donor	Donor_structure	Acceptor	Acceptor_structure	PCE (%)	Test order
111	PM7	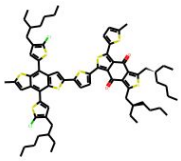	Y6		15.12	18
115	PBDTCl-TZ	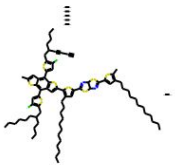	IT-4F	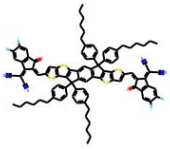	12.21	19
114	PBDTSi-TZ	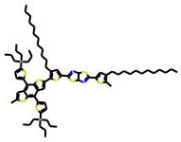	IT-4F	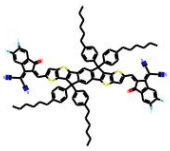	11.26	20
28	PBDBTz-5	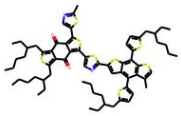	IT-4F	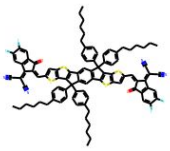	9.60	21
16	PM6	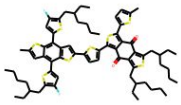	ID-4F	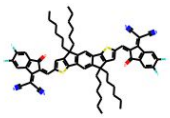	6.40	22
105	PBDB-T-2Cl	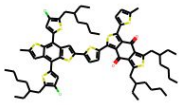	FOIC	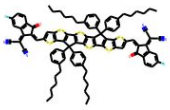	5.75	23
116	PFBCPZ	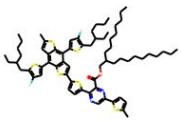	IT-4F	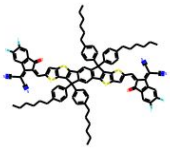	15.30	24
117	PTQ7	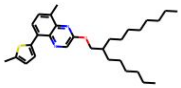	Y6	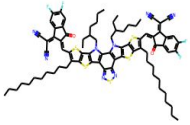	5.75	25
161	PBFB-T-SF	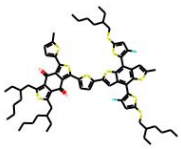	IT-4F	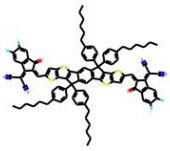	12.97	26

Index No.	Donor	Donor_structure	Acceptor	Acceptor_structure	PCE (%)	Test order
174	PBDB-T-SF	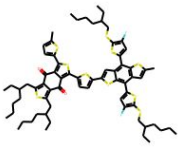	IT-4F	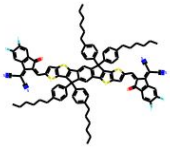	13.10	27
127	C1	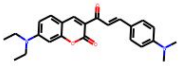	IT-4F	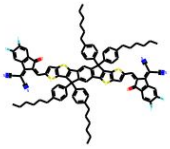	8.31	28
22	PM6	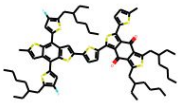	IT-4F	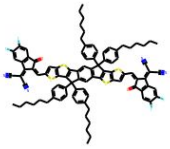	12.90	29
26	PBDB-T	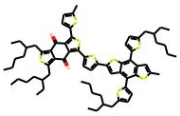	IT-4F	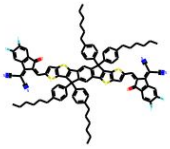	9.30	30
61	PM6	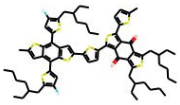	3TP3T-4F	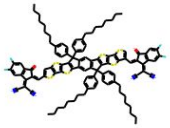	13.70	31
199	PM6	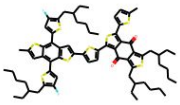	DTC-4F	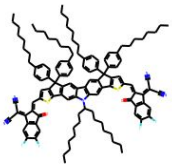	13.37	32
157	PBDB-TF	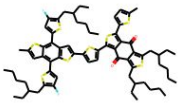	IE-4F	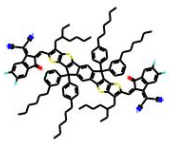	9.30	33
83	PBDB-TF	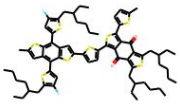	BTP-6F	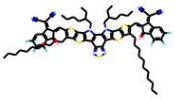	15.30	34
7	D-2F	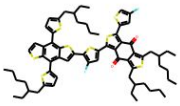	IT-4F	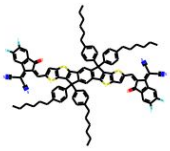	10.90	35

Index No.	Donor	Donor_structure	Acceptor	Acceptor_structure	PCE (%)	Test order
59	PBDB-TF	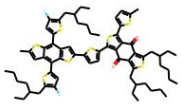	Aqx-2	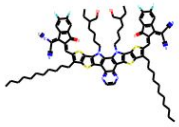	16.64	36
58	PBDB-TF	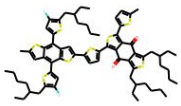	AQx-1	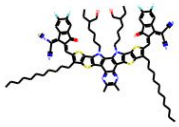	13.31	37
30	PM6	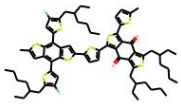	Y6	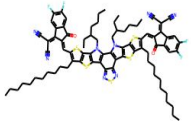	15.00	38
77	PM6	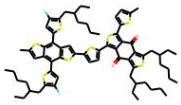	Y18	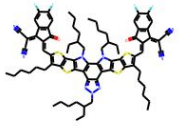	13.32	39
171	PM6	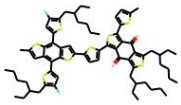	L8-BO	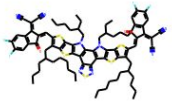	18.32	40

Table S4 D:A combination selected by MEI acquisition function with corresponding test order. Best candidate is discovered in 24 iterations, and 15% PCE is crossed in 19 iterations.

Index No.	Donor	Donor_structure	Acceptor	Acceptor_structure	PCE (%)	Test order
54	PffBT2T-TT	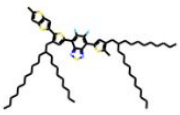	O-IDTBR	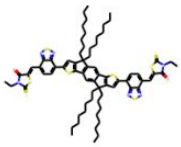	10.10	1
36	PvBDTTAZ	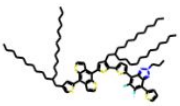	O-IDTBR	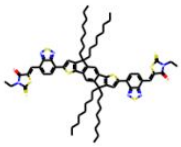	11.40	2

Index No.	Donor	Donor_structure	Acceptor	Acceptor_structure	PCE (%)	Test order
112	DR3TBDTT	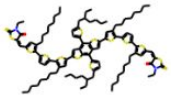	O-IDTBR	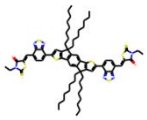	4.12	3
129	J71	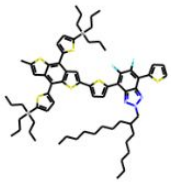	IDTT-BH	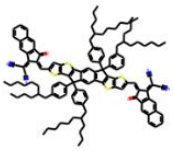	11.05	4
144	J71	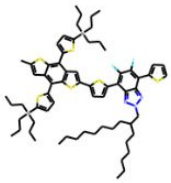	m-MeIC	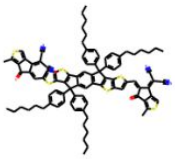	11.73	5
103	J71	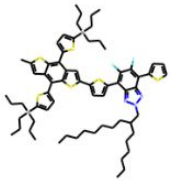	FOIC	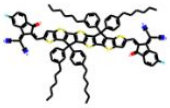	8.48	6
60	J61	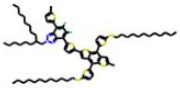	BTA3	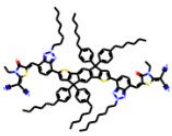	8.25	7
80	PBT1-C	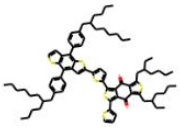	IDTT-C10-TIC	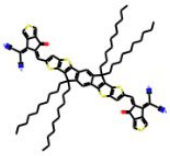	12.50	8
79	PBT1-C	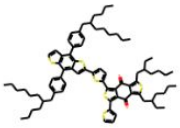	IDTT-C8-TIC	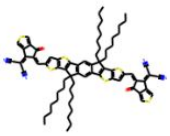	13.40	9
78	PBT1-C	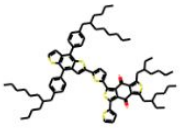	IDTT-C6-TIC	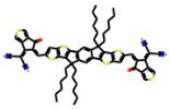	9.60	10
0	D-0F	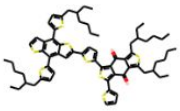	C8-ITIC	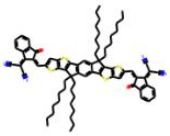	11.60	11

Index No.	Donor	Donor_structure	Acceptor	Acceptor_structure	PCE (%)	Test order
181	PBDB-T	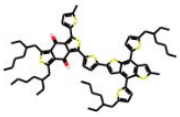	FDICTF	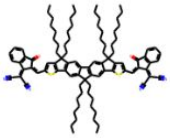	9.81	12
52	PBT1-C	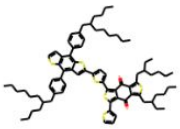	BTA3	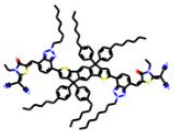	8.10	13
114	PBDTSi-TZ	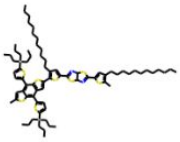	IT-4F	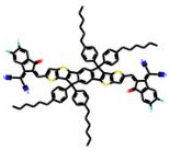	11.26	14
113	BTTzR	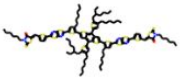	Y6	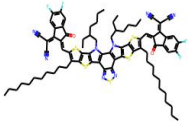	13.90	15
75	PE71	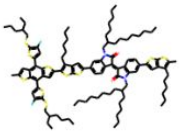	Y6	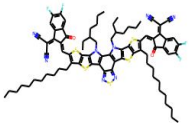	12.03	16
76	PE72	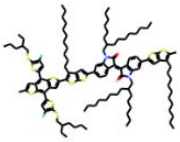	Y6	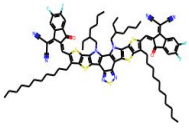	9.74	17
117	PTQ7	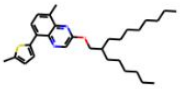	Y6	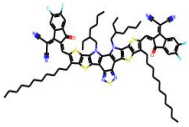	5.75	18
111	PM7	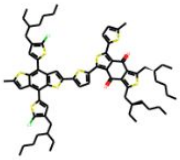	Y6	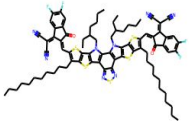	15.12	19
67	PBDBT-2Cl	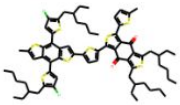	IT-4F	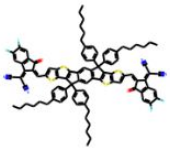	14.16	20

Index No.	Donor	Donor_structure	Acceptor	Acceptor_structure	PCE (%)	Test order
121	L2		TT-PT-T-4F	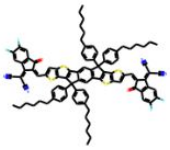	14.00	21
115	PBDTCl-TZ	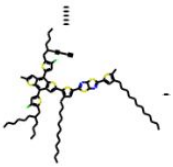	IT-4F	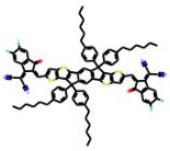	12.21	22
30	PM6	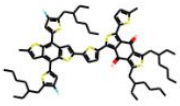	Y6	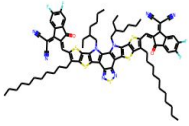	15.00	23
171	PM6	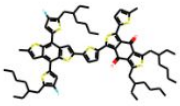	L8-BO	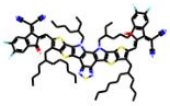	18.32	24

Table S5 D:A combination selected by MLI acquisition function with corresponding test order. Best candidate is discovered in 17 iterations, and 15% PCE is crossed in 13 iterations.

Index No.	Donor	Donor_structure	Acceptor	Acceptor_structure	PCE (%)	Test order
54	PffBT2T-TT	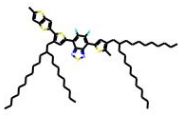	O-IDTBR	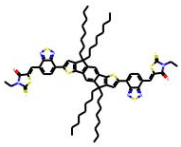	10.10	1
74	PTB7-Th	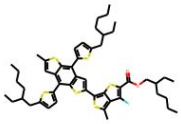	IDT-2BR	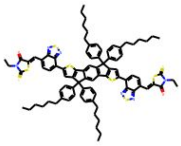	6.19	2
36	PvBDTTAZ	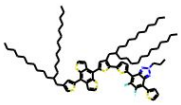	O-IDTBR	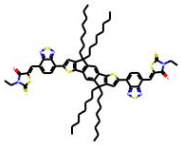	11.40	3

Index No.	Donor	Donor_structure	Acceptor	Acceptor_structure	PCE (%)	Test order
112	DR3TBDTT	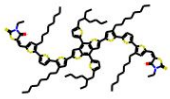	O-IDTBR	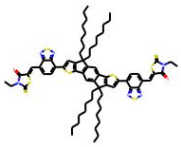	4.12	4
117	PTQ7	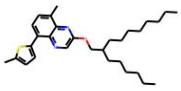	Y6	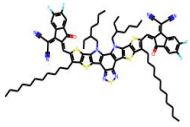	5.75	5
153	FTAZ	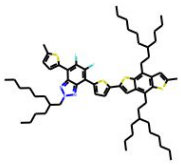	INIC1	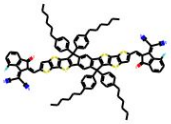	10.10	6
79	PBT1-C	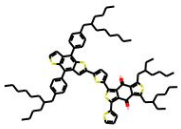	IDTT-C8-TIC	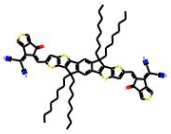	13.40	7
80	PBT1-C	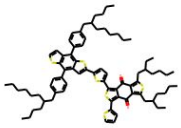	IDTT-C10-TIC	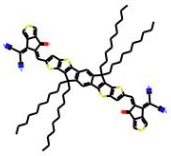	12.50	8
78	PBT1-C	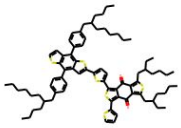	IDTT-C6-TIC	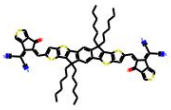	9.60	9
52	PBT1-C	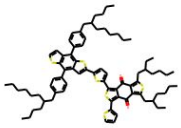	BTA3	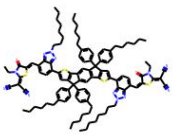	8.10	10
66	PBDB-T	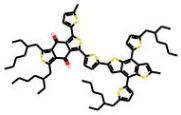	DOC2C6-2F	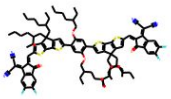	13.24	11
43	PBDB-T	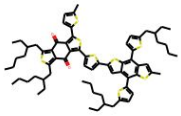	BTOR-IC4F	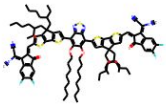	11.48	12

Index No.	Donor	Donor_structure	Acceptor	Acceptor_structure	PCE (%)	Test order
111	PM7	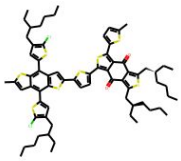	Y6		15.12	13
30	PM6	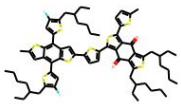	Y6		15.00	14
77	PM6	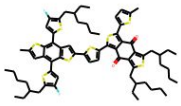	Y18	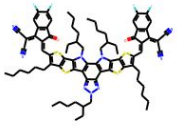	13.32	15
124	PM6	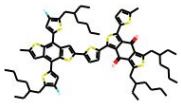	ABP4T-4F	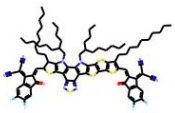	15.20	16
171	PM6	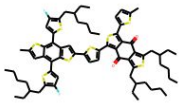	L8-BO	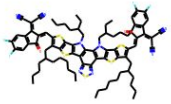	18.32	17

Table S6 D:A combination selected by MU acquisition function with corresponding test order. Best candidate is discovered in 44 iterations, and 15% PCE is crossed in 24 iterations.

Index No.	Donor	Donor_structure	Acceptor	Acceptor_structure	PCE (%)	Test order
92	PTH37	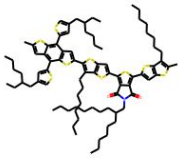	i-IEICO	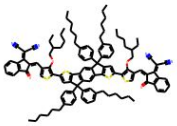	4.46	1
165	PTH37	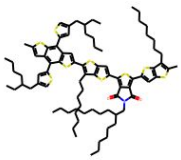	ITIC	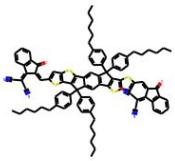	10.90	2

Index No.	Donor	Donor_structure	Acceptor	Acceptor_structure	PCE (%)	Test order
186	PBDB-T	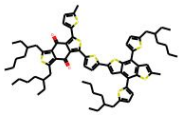	IDT-T-N	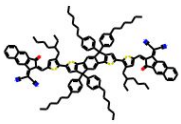	5.40	3
156	PBDB-T	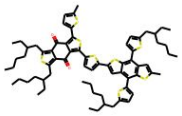	IEIC	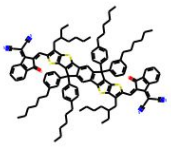	7.30	4
106	PMT49	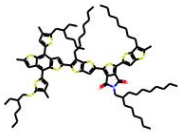	FOIC	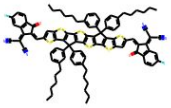	9.11	5
93	PMT49	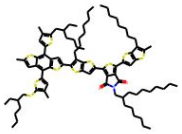	i-IEICO	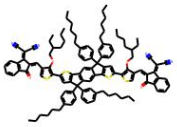	4.11	6
108	PMT49	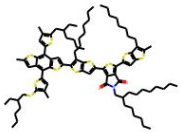	Y6	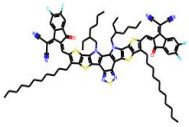	10.81	7
64	PBDB-T	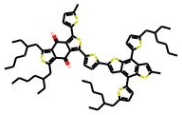	DOC8-IC	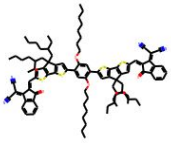	9.41	8
101	PMT49	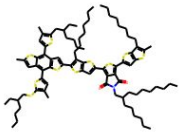	IEICO-4F		4.50	9
195	J73		m-ITIC	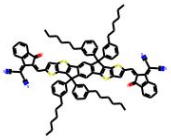	10.71	10
129	J71	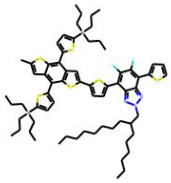	IDTT-BH	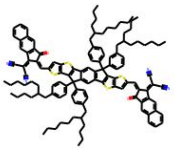	11.05	11

Index No.	Donor	Donor_structure	Acceptor	Acceptor_structure	PCE (%)	Test order
130	J71	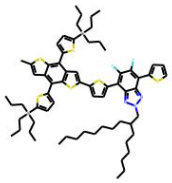	IDTT-OBH	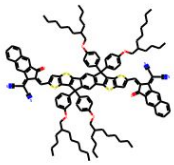	8.02	12
44	PTB7-Th	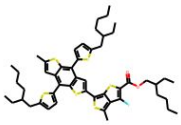	IOTIC	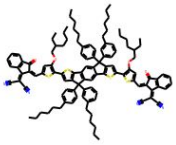	6.00	13
60	J61	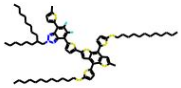	BTA3	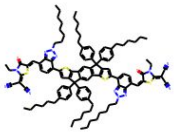	8.25	14
131	PDCBT	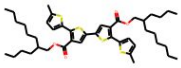	IDTT-BH		10.35	15
76	PE72	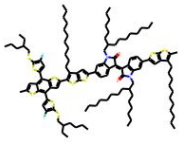	Y6	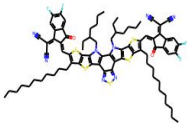	9.74	16
172	PBDTT-DPP		IEICO-4F	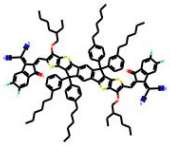	8.14	17
66	PBDB-T	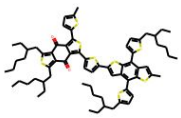	DOC2C6-2F	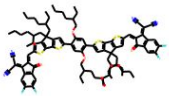	13.24	18
43	PBDB-T	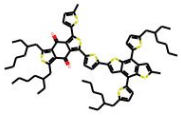	BTOR-IC4F	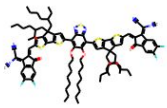	11.48	19
84	PTH37	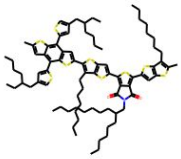	i-IEICO-4F	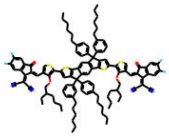	9.64	20

Index No.	Donor	Donor_structure	Acceptor	Acceptor_structure	PCE (%)	Test order
85	PMT49	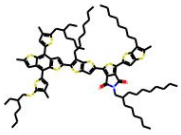	i-IEICO-4F	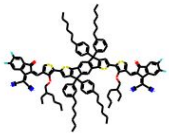	9.82	21
88	PTH37	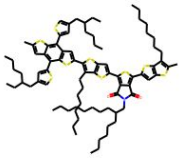	i-IEICO-2F	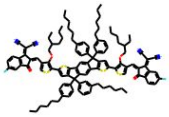	8.16	22
158	PBDB-T	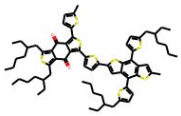	IE-4F	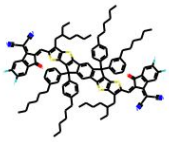	10.80	23
122	PM6	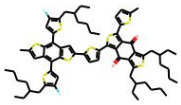	BP4T-4F	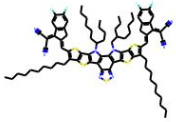	17.10	24
83	PBDB-TF	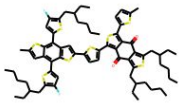	BTP-6F	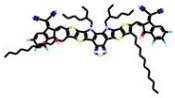	15.30	25
47	PBDB-TF	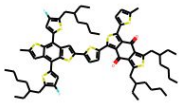	BTP-eC7		14.90	26
126	PBDB-TF	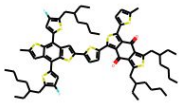	3TT-OCIC	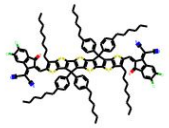	12.43	27
125	PBDB-TF	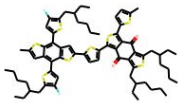	F-2Cl	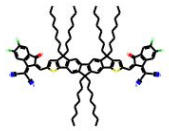	12.87	28
14	PM6	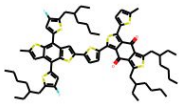	Y11	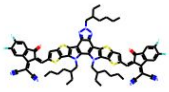	13.80	29

Index No.	Donor	Donor_structure	Acceptor	Acceptor_structure	PCE (%)	Test order
62	PM6	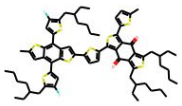	3TP3T-IC	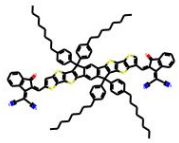	8.90	30
81	PBDB-TF	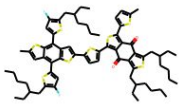	BTP-0F	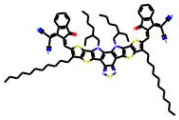	8.20	31
82	PBDB-TF	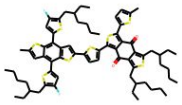	BTP-2F	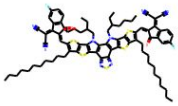	14.10	32
180	PBDB-T	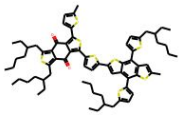	DICTF	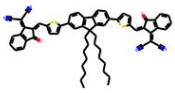	5.65	33
12	PBDB-T	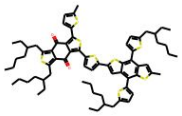	Y2	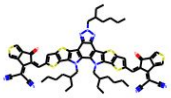	13.40	34
179	PTB7-Th	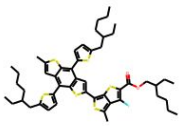	DICTF	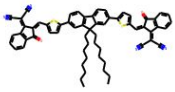	6.54	35
123	PM6	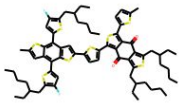	BP5T-4F		16.70	36
162	PTB7-Th	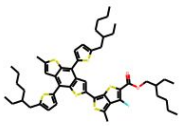	SCPDT-PDI4	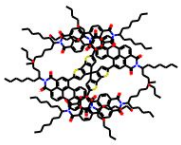	7.11	37
59	PBDB-TF	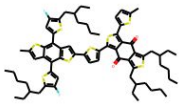	Aqx-2	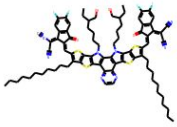	16.64	38

Index No.	Donor	Donor_structure	Acceptor	Acceptor_structure	PCE (%)	Test order
124	PM6	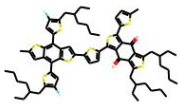	ABP4T-4F	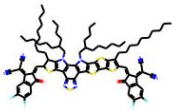	15.20	39
42	PBDB-T	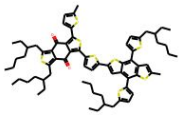	BT2F-IC4F	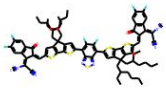	8.45	40
199	PM6	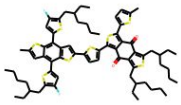	DTC-4F	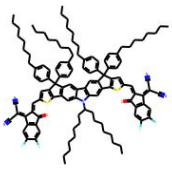	13.37	41
16	PM6	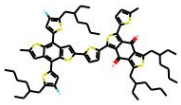	ID-4F	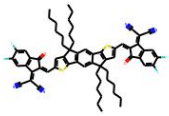	6.40	42
15	PM6	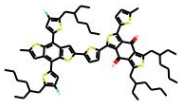	IDST-4F	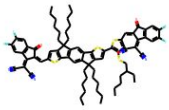	14.30	43
171	PM6	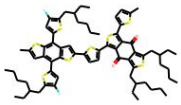	L8-BO	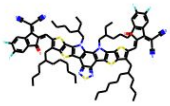	18.32	44

Table S7 D:A combination selected by UCB acquisition function with corresponding test order. Best candidate is discovered in 30 iterations, and 15% PCE is crossed in 22 iterations.

Index No.	Donor	Donor_structure	Acceptor	Acceptor_structure	PCE (%)	Test order
54	PffBT2T-TT	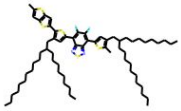	O-IDTBR	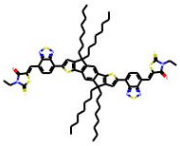	10.10	1

Index No.	Donor	Donor_structure	Acceptor	Acceptor_structure	PCE (%)	Test order
74	PTB7-Th	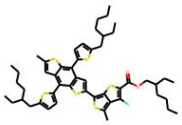	IDT-2BR	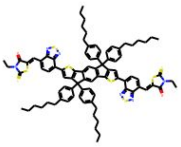	6.19	2
36	PvBDTTAZ	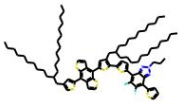	O-IDTBR	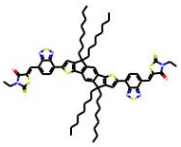	11.40	3
112	DR3TBDTT	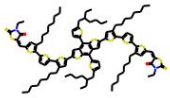	O-IDTBR	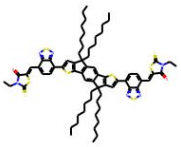	4.12	4
117	PTQ7	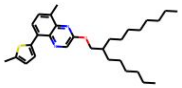	Y6	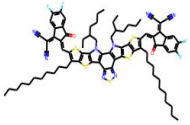	5.75	5
129	J71	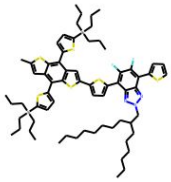	IDTT-BH		11.05	6
144	J71	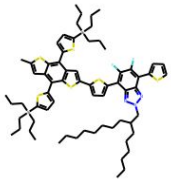	m-MeIC	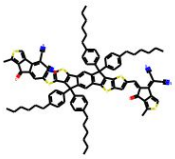	11.73	7
103	J71	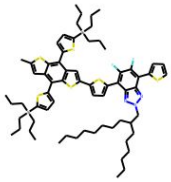	FOIC	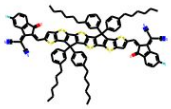	8.48	8
31	J52		BTA3	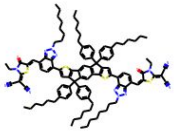	9.41	9
56	J71	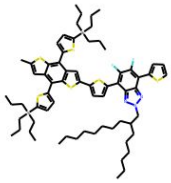	ZITI-C	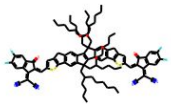	13.18	10

Index No.	Donor	Donor_structure	Acceptor	Acceptor_structure	PCE (%)	Test order
55	J71	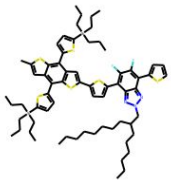	ZITI-S	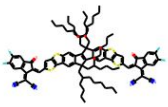	9.12	11
57	J71	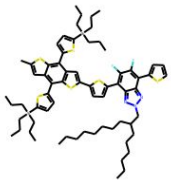	ZITI-N	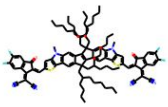	13.68	12
97	J71	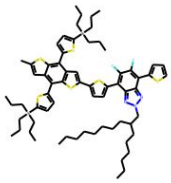	i-IEICO-4F	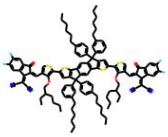	8.72	13
130	J71	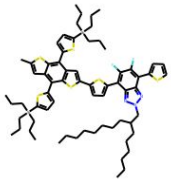	IDTT-OBH	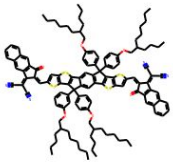	8.02	14
181	PBDB-T	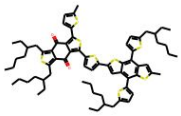	FDICTF	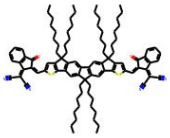	9.81	15
80	PBT1-C	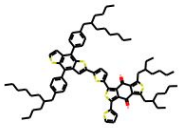	IDTT-C10-TIC	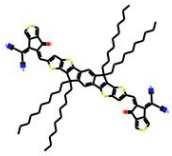	12.50	16
79	PBT1-C	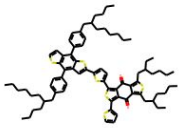	IDTT-C8-TIC	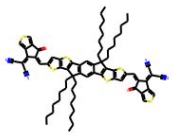	13.40	17
78	PBT1-C	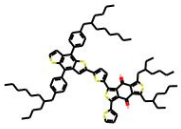	IDTT-C6-TIC	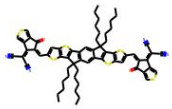	9.60	18
0	D-0F	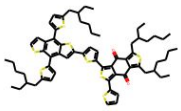	C8-ITIC	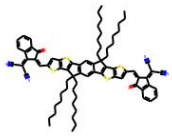	11.60	19

Index No.	Donor	Donor_structure	Acceptor	Acceptor_structure	PCE (%)	Test order
66	PBDB-T	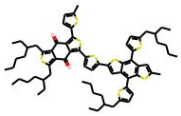	DOC2C6-2F	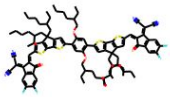	13.24	20
43	PBDB-T	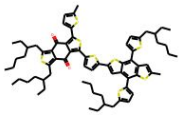	BTOR-IC4F	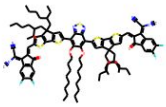	11.48	21
59	PBDB-TF	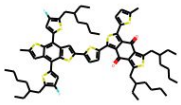	Aqx-2	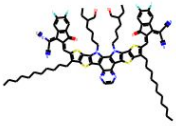	16.64	22
58	PBDB-TF	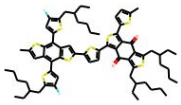	AQx-1	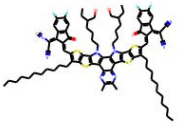	13.31	23
77	PM6	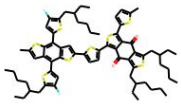	Y18	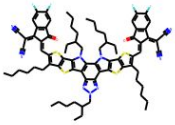	13.32	24
14	PM6	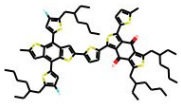	Y11	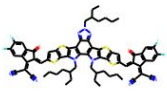	13.80	25
42	PBDB-T	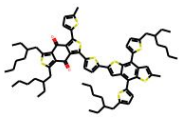	BT2F-IC4F	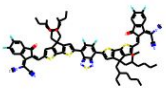	8.45	26
111	PM7	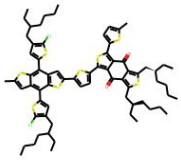	Y6		15.12	27
124	PM6	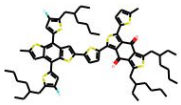	ABP4T-4F	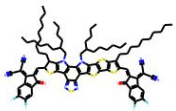	15.20	28

Index No.	Donor	Donor_structure	Acceptor	Acceptor_structure	PCE (%)	Test order
75	PE71	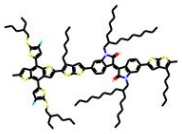	Y6		12.03	29
171	PM6	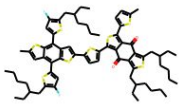	L8-BO	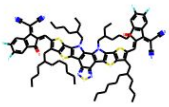	18.32	30

Table S8 Randomly chosen initial training set with PCE less than 10% for 1318 dataset

S. No	PCE (%)
1	0.50
2	0.30
3	1.42
4	0.76
5	0.77
6	4.81
7	6.50
8	4.68
9	5.60
10	2.11

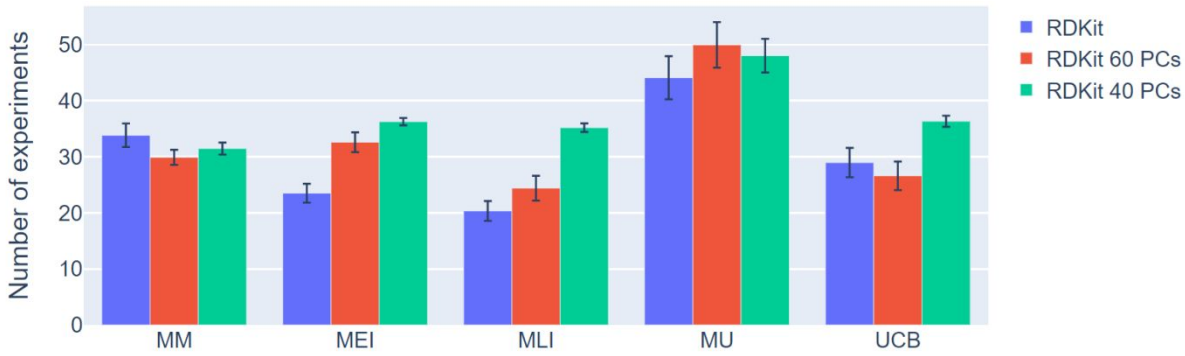

Figure S2 Bars represent number of experiments carried out to discover the best candidate in search space using random forest with RDKit descriptors. Blue bars represents result for training set with all descriptors after feature engineering, red bars represents result for training set with 60 PCs, and green bars represents result for training set with 40 PCs.

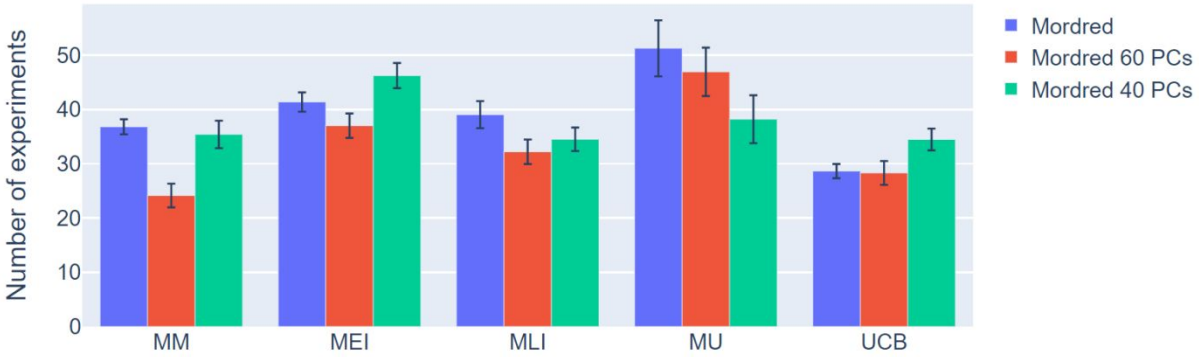

Figure S3 Bars represent number of experiments carried out to discover the best candidate in search space using random forest with mordred descriptors. Blue bars represents result for training set with all descriptors after feature engineering, red bars represents result for training set with 60 PCs, and green bars represents result for training set with 40 PCs.

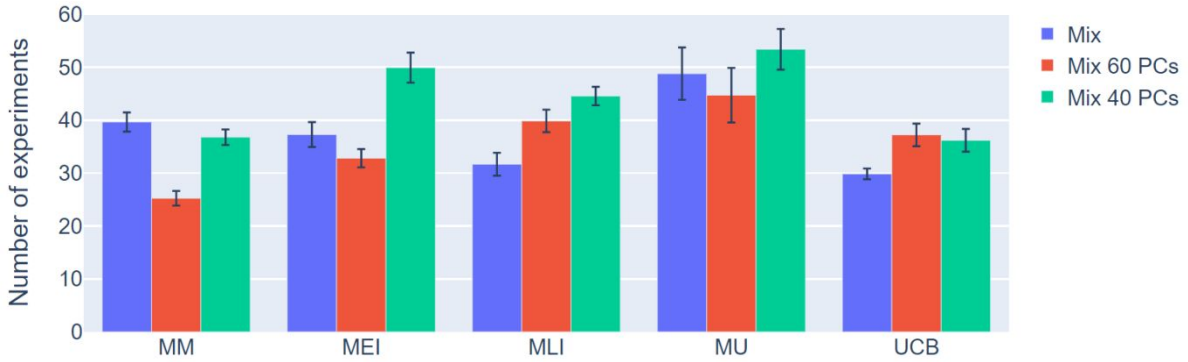

Figure S4 Bars represent number of experiments carried out to discover the best candidate in search space using random forest with mix of RDKit and mordred descriptors. Blue bars represents result for training set with all descriptors after feature engineering, red bars represents result for training set with 60 PCs, and green bars represents result for training set with 40 PCs.

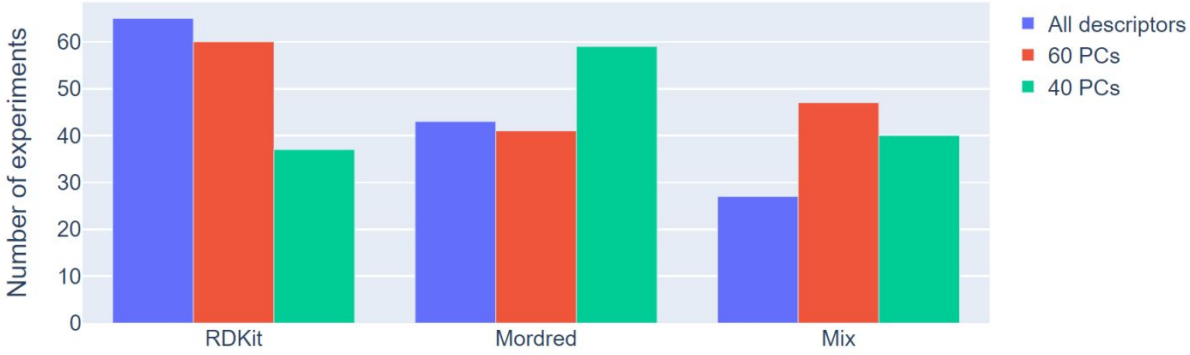

Figure S5 Bars represent number of experiments carried out to discover the best candidate in search space using gaussian process regressor (GPR) with RDKit descriptors, Mordred descriptors, and mix of both. Blue bars represents result for training set with all descriptors after feature engineering, red bars represents result for training set with 60 PCs, and green bars represents result for training set with 40 PCs.

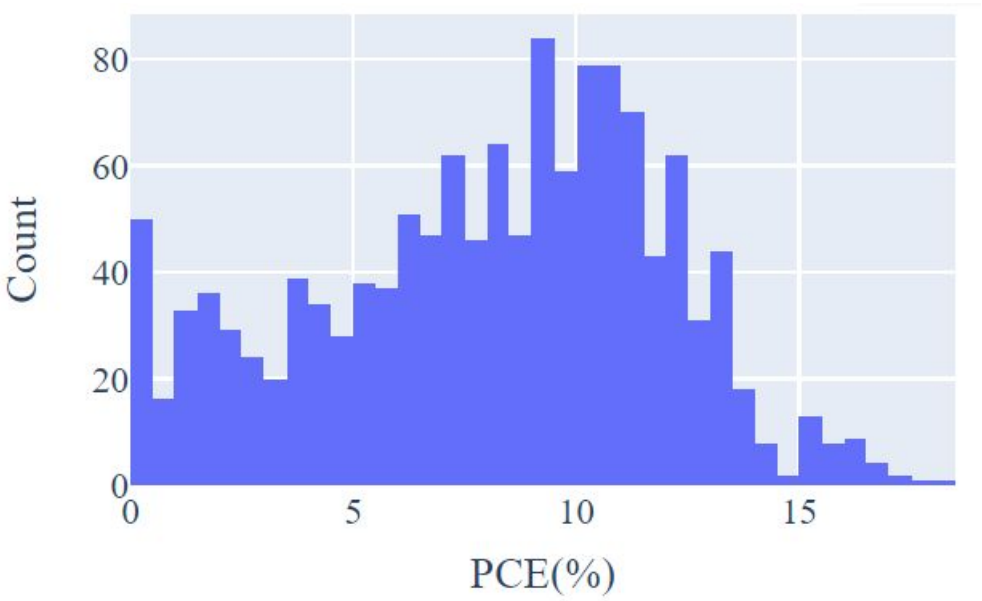

Figure S6 PCE distribution for 1318 unique D:A combination[76]

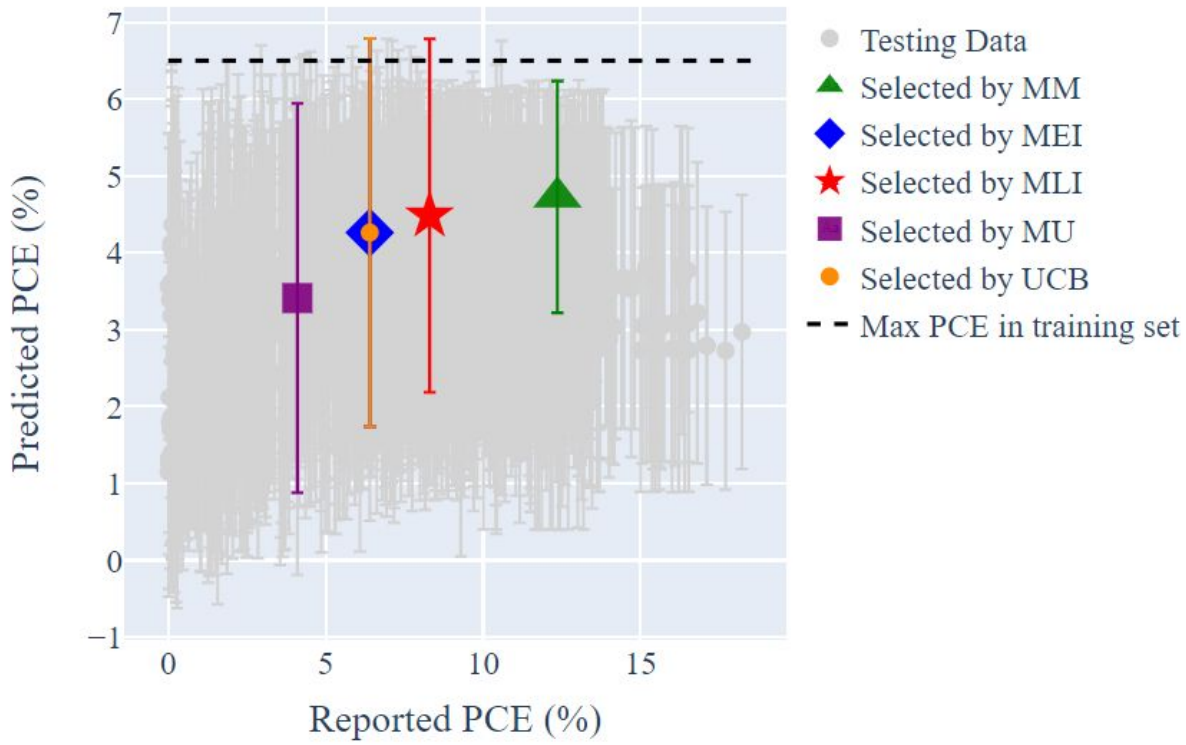

Figure S7 Illustration of first iteration results for 1318 dataset. Predictions of random forest model trained on randomly selected data (table 3) along with sample-wise uncertainty estimates are represented in grey. In the first iteration, candidates selected by MM, MEI, MLI, MU, and UCB acquisition function are colored, and error bar represents observational uncertainty. Dotted line represents the maximum PCE in the training set. Acquisition functions that combine both exploration and exploitation (MEI, MLI, and UCB) outperform pure exploitation (MM) and pure exploration (MU).

REFERENCES

(1) Eisner, F. D.; Azzouzi, M.; Fei, Z.; Hou, X.; Anthopoulos, T. D.; Dennis, T. J. S.; Heeney, M.; Nelson, J. Hybridization of Local Exciton and Charge-Transfer States Reduces Nonradiative Voltage Losses in Organic Solar Cells. *J. Am. Chem. Soc.* **2019**, *141* (15), 6362–6374. https://doi.org/10.1021/jacs.9b01465.

(2) Baran, D.; Kirchartz, T.; Wheeler, S.; Dimitrov, S.; Abdelsamie, M.; Gorman, J.; Ashraf, R. S.; Holliday, S.; Wadsworth, A.; Gasparini, N.; Kaienburg, P.; Yan, H.; Amassian, A.; Brabec, C. J.; Durrant, J. R.; McCulloch, I. Reduced Voltage Losses Yield 10% Efficient Fullerene Free Organic Solar Cells with >1 V Open Circuit Voltages. *Energy Environ. Sci.* **2016**, *9* (12), 3783–3793. https://doi.org/10.1039/C6EE02598F.

(3) Yuan, J.; Huang, T.; Cheng, P.; Zou, Y.; Zhang, H.; Yang, J. L.; Chang, S. Y.; Zhang, Z.; Huang, W.; Wang, R.; Meng, D.; Gao, F.; Yang, Y. Enabling Low Voltage Losses and High Photocurrent in Fullerene-Free Organic Photovoltaics. *Nat. Commun.* **2019**, *10* (1), 1–8.

https://doi.org/10.1038/s41467-019-08386-9.

(4) Liu, J.; Chen, S.; Qian, D.; Gautam, B.; Yang, G.; Zhao, J.; Bergqvist, J.; Zhang, F.; Ma, W.; Ade, H.; Inganäs, O.; Gundogdu, K.; Gao, F.; Yan, H. Fast Charge Separation in a Non-Fullerene Organic Solar Cell with a Small Driving Force. *Nat. Energy* **2016**, *1* (7), 16089. https://doi.org/10.1038/nenergy.2016.89.

(5) Liu, S.; Yuan, J.; Deng, W.; Luo, M.; Xie, Y.; Liang, Q.; Zou, Y.; He, Z.; Wu, H.; Cao, Y. High-Efficiency Organic Solar Cells with Low Non-Radiative Recombination Loss and Low Energetic Disorder. *Nat. Photonics* **2020**, *14* (5), 300–305. https://doi.org/10.1038/s41566-019-0573-5.

(6) Guo, Q.; Lin, J.; Liu, H.; Dong, X.; Guo, X.; Ye, L.; Ma, Z.; Tang, Z.; Ade, H.; Zhang, M.; Li, Y. Asymmetrically Noncovalently Fused-Ring Acceptor for High-Efficiency Organic Solar Cells with Reduced Voltage Loss and Excellent Thermal Stability. *Nano Energy* **2020**, *74*, 104861. https://doi.org/10.1016/j.nanoen.2020.104861.

(7) Liu, X.; Du, X.; Wang, J.; Duan, C.; Tang, X.; Heumueller, T.; Liu, G.; Li, Y.; Wang, Z.; Wang, J.; Liu, F.; Li, N.; Brabec, C. J.; Huang, F.; Cao, Y. Efficient Organic Solar Cells with Extremely High Open-Circuit Voltages and Low Voltage Losses by Suppressing Nonradiative Recombination Losses. *Adv. Energy Mater.* **2018**, *8* (26), 1801699. https://doi.org/10.1002/aenm.201801699.

(8) Gao, W.; Liu, T.; Sun, R.; Zhang, G.; Xiao, Y.; Ma, R.; Zhong, C.; Lu, X.; Min, J.; Yan, H.; Yang, C. Dithieno[3,2- B :2′,3′- d]Pyrrol-Fused Asymmetrical Electron Acceptors: A Study into the Effects of Nitrogen-Functionalization on Reducing Nonradiative Recombination Loss and Dipole Moment on Morphology. *Adv. Sci.* **2020**, *7* (5), 1902657. https://doi.org/10.1002/advs.201902657.

(9) Luo, Z.; Liu, T.; Wang, Y.; Zhang, G.; Sun, R.; Chen, Z.; Zhong, C.; Wu, J.; Chen, Y.; Zhang, M.; Zou, Y.; Ma, W.; Yan, H.; Min, J.; Li, Y.; Yang, C. Reduced Energy Loss Enabled by a Chlorinated Thiophene-Fused Ending-Group Small Molecular Acceptor for Efficient Nonfullerene Organic Solar Cells with 13.6% Efficiency. *Adv. Energy Mater.* **2019**, *9* (18), 1900041. https://doi.org/10.1002/aenm.201900041.

(10) Xie, Y.; Li, T.; Guo, J.; Bi, P.; Xue, X.; Ryu, H. S.; Cai, Y.; Min, J.; Huo, L.; Hao, X.; Woo, H. Y.; Zhan, X.; Sun, Y. Ternary Organic Solar Cells with Small Nonradiative Recombination Loss. *ACS Energy Lett.* **2019**, *4* (5), 1196–1203. https://doi.org/10.1021/acsenergylett.9b00681.

(11) Cui, Y.; Yao, H.; Zhang, J.; Zhang, T.; Wang, Y.; Hong, L.; Xian, K.; Xu, B.; Zhang, S.; Peng, J.; Wei, Z.; Gao, F.; Hou, J. Over 16% Efficiency Organic Photovoltaic Cells Enabled by a Chlorinated Acceptor with Increased Open-Circuit Voltages. *Nat. Commun.* **2019**, *10* (1), 2515. https://doi.org/10.1038/s41467-019-10351-5.

(12) Zhang, L.; Deng, W.; Wu, B.; Ye, L.; Sun, X.; Wang, Z.; Gao, K.; Wu, H.; Duan, C.; Huang, F.; Cao, Y. Reduced Energy Loss in Non-Fullerene Organic Solar Cells with Isomeric Donor Polymers Containing Thiazole π-Spacers. *ACS Appl. Mater. Interfaces* **2020**, *12* (1), 753–762. https://doi.org/10.1021/acsami.9b18048.

(13) Gao, B.; Yao, H.; Hong, L.; Hou, J. Efficient Organic Solar Cells with a High Open-Circuit Voltage of 1.34 V. *Chinese J. Chem.* **2019**, *37* (11), 1153–1157. https://doi.org/10.1002/cjoc.201900269.

(14) Karki, A.; Vollbrecht, J.; Dixon, A. L.; Schopp, N.; Schrock, M.; Reddy, G. N. M.; Nguyen, T. Q. Understanding the High Performance of over 15% Efficiency in Single-Junction Bulk Heterojunction Organic Solar Cells. *Adv. Mater.* **2019**, *31* (48), 1–9. https://doi.org/10.1002/adma.201903868.

(15) Tang, A.; Song, W.; Xiao, B.; Guo, J.; Min, J.; Ge, Z.; Zhang, J.; Wei, Z.; Zhou, E. Benzotriazole-Based Acceptor and Donors, Coupled with Chlorination, Achieve a High V OC of 1.24 V and an Efficiency of 10.5% in Fullerene-Free Organic Solar Cells. *Chem. Mater.* **2019**, *31* (11), 3941–3947. https://doi.org/10.1021/acs.chemmater.8b05316.

(16) Qian, D.; Zheng, Z.; Yao, H.; Tress, W.; Hopper, T. R.; Chen, S.; Li, S.; Liu, J.; Chen, S.; Zhang, J.; Liu, X.-K.; Gao, B.; Ouyang, L.; Jin, Y.; Pozina, G.; Buyanova, I. A.; Chen, W. M.; Inganäs, O.; Coropceanu, V.; Bredas, J.-L.; Yan, H.; Hou, J.; Zhang, F.; Bakulin, A. A.; Gao, F. Design Rules for Minimizing Voltage Losses in High-Efficiency Organic Solar Cells. *Nat. Mater.* **2018**, *17* (8), 703–709. https://doi.org/10.1038/s41563-018-0128-z.

(17) Zhang, J.; Kan, B.; Pearson, A. J.; Parnell, A. J.; Cooper, J. F. K.; Liu, X.-K.; Conaghan, P. J.; Hopper, T. R.; Wu, Y.; Wan, X.; Gao, F.; Greenham, N. C.; Bakulin, A. A.; Chen, Y.; Friend, R. H. Efficient Non-Fullerene Organic Solar Cells Employing Sequentially Deposited Donor–Acceptor Layers. *J. Mater. Chem. A* **2018**, *6* (37), 18225–18233. https://doi.org/10.1039/C8TA06860G.

(18) Yang, F.; Qian, D.; Balawi, A. H.; Wu, Y.; Ma, W.; Laquai, F.; Tang, Z.; Zhang, F.; Li, W. Performance Limitations in Thieno[3,4-c]Pyrrole-4,6-Dione-Based Polymer:ITIC Solar Cells. *Phys. Chem. Chem. Phys.* **2017**, *19* (35), 23990–23998. https://doi.org/10.1039/c7cp04780k.

(19) Wang, Y.; Liu, Z.; Cui, X.; Wang, C.; Lu, H.; Liu, Y.; Fei, Z.; Ma, Z.; Bo, Z. Small Molecule Acceptors with a Ladder-like Core for High-Performance Organic Solar Cells with Low Non-Radiative Energy Losses. *J. Mater. Chem. A* **2020**, *8* (25), 12495–12501. https://doi.org/10.1039/D0TA03683H.

(20) Karki, A.; Vollbrecht, J.; Gillett, A. J.; Selter, P.; Lee, J.; Peng, Z.; Schopp, N.; Dixon, A. L.; Schrock, M.; Nádaždy, V.; Schauer, F.; Ade, H.; Chmelka, B. F.; Bazan, G. C.; Friend, R. H.; Nguyen, T.-Q. Unifying Charge Generation, Recombination, and Extraction in Low-Offset Non-Fullerene Acceptor Organic Solar Cells. *Adv. Energy Mater.* **2020**, *10* (29), 2001203. https://doi.org/10.1002/aenm.202001203.

(21) Cui, Y.; Yao, H.; Zhang, J.; Xian, K.; Zhang, T.; Hong, L.; Wang, Y.; Xu, Y.; Ma, K.; An, C.; He, C.; Wei, Z.; Gao, F.; Hou, J. Single-Junction Organic Photovoltaic Cells with Approaching 18% Efficiency. *Adv. Mater.* **2020**, *32* (19), 1–7. https://doi.org/10.1002/adma.201908205.

(22) Sharma, R.; Jain, N.; Lee, H.; Kabra, D.; Yoo, S. Comprehensive and Comparative Analysis of Photoinduced Charge Generation, Recombination Kinetics, and Energy Losses in Fullerene and Nonfullerene Acceptor-Based Organic Solar Cells. *ACS Appl. Mater. Interfaces* **2020**, *12* (40), 45083–45091. https://doi.org/10.1021/acsami.0c13579.

(23) An, N.; Cai, Y.; Wu, H.; Tang, A.; Zhang, K.; Hao, X.; Ma, Z.; Guo, Q.; Ryu, H. S.; Woo, H. Y.; Sun, Y.; Zhou, E. Solution-Processed Organic Solar Cells with High Open-Circuit Voltage of 1.3 V and Low Non-Radiative Voltage Loss of 0.16 V. *Adv. Mater.* **2020**, *2002122*, 1–7. https://doi.org/10.1002/adma.202002122.

(24) Chen, S.; Wang, Y.; Zhang, L.; Zhao, J.; Chen, Y.; Zhu, D.; Yao, H.; Zhang, G.; Ma, W.; Friend, R. H.; Chow, P. C. Y.; Gao, F.; Yan, H. Efficient Nonfullerene Organic Solar Cells with Small Driving Forces for Both Hole and Electron Transfer. *Adv. Mater.* **2018**, *30* (45), 1–7. https://doi.org/10.1002/adma.201804215.

(25) Zhang, J.; Liu, W.; Zhang, M.; Liu, Y.; Zhou, G.; Xu, S.; Zhang, F.; Zhu, H.; Liu, F.; Zhu, X. Revealing the Critical Role of the HOMO Alignment on Maximizing Current Extraction and Suppressing Energy Loss in Organic Solar Cells. *iScience* **2019**, *19*, 883–893. https://doi.org/10.1016/j.isci.2019.08.038.

(26) Zhou, Z.; Liu, W.; Zhou, G.; Zhang, M.; Qian, D.; Zhang, J.; Chen, S.; Xu, S.; Yang, C.; Gao, F.;

Zhu, H.; Liu, F.; Zhu, X. Subtle Molecular Tailoring Induces Significant Morphology Optimization Enabling over 16% Efficiency Organic Solar Cells with Efficient Charge Generation. *Adv. Mater.* **2020**, *32* (4), 1906324. https://doi.org/10.1002/adma.201906324.

(27) Tang, A.; Xiao, B.; Wang, Y.; Gao, F.; Tajima, K.; Bin, H.; Zhang, Z.; Li, Y.; Wei, Z.; Zhou, E. Simultaneously Achieved High Open-Circuit Voltage and Efficient Charge Generation by Fine-Tuning Charge-Transfer Driving Force in Nonfullerene Polymer Solar Cells. *Adv. Funct. Mater.* **2018**, *28* (6), 1704507. https://doi.org/10.1002/adfm.201704507.

(28) Song, J.; Li, C.; Zhu, L.; Guo, J.; Xu, J.; Zhang, X.; Weng, K.; Zhang, K.; Min, J.; Hao, X.; Zhang, Y.; Liu, F.; Sun, Y. Ternary Organic Solar Cells with Efficiency >16.5% Based on Two Compatible Nonfullerene Acceptors. *Adv. Mater.* **2019**, *31* (52), 1–9. https://doi.org/10.1002/adma.201905645.

(29) Huang, H.; Guo, Q.; Feng, S.; Zhang, C.; Bi, Z.; Xue, W.; Yang, J.; Song, J.; Li, C.; Xu, X.; Tang, Z.; Ma, W.; Bo, Z. Noncovalently Fused-Ring Electron Acceptors with near-Infrared Absorption for High-Performance Organic Solar Cells. *Nat. Commun.* **2019**, *10* (1), 3038. https://doi.org/10.1038/s41467-019-11001-6.

(30) Zhang, X.; Yao, N.; Wang, R.; Li, Y.; Zhang, D.; Wu, G.; Zhou, J.; Li, X.; Zhang, H.; Zhang, J.; Wei, Z.; Zhang, C.; Zhou, H.; Zhang, F.; Zhang, Y. On the Understanding of Energy Loss and Device Fill Factor Trade-Offs in Non-Fullerene Organic Solar Cells with Varied Energy Levels. *Nano Energy* **2020**, *75* (March), 105032. https://doi.org/10.1016/j.nanoen.2020.105032.

(31) Saito, T.; Natsuda, S.; Imakita, K.; Tamai, Y.; Ohkita, H. Role of Energy Offset in Nonradiative Voltage Loss in Organic Solar Cells. *Sol. RRL* **2020**, *4* (9), 2000255. https://doi.org/10.1002/solr.202000255.

(32) Zhang, B.; An, N.; Wu, H.; Geng, Y.; Sun, Y.; Ma, Z.; Li, W.; Guo, Q.; Zhou, E. The First Application of Isoindigo-Based Polymers in Non-Fullerene Organic Solar Cells. *Sci. China Chem.* **2020**, *63* (9), 1262–1271. https://doi.org/10.1007/s11426-020-9777-1.

(33) Zhu, C.; Yuan, J.; Cai, F.; Meng, L.; Zhang, H.; Chen, H.; Li, J.; Qiu, B.; Peng, H.; Chen, S.; Hu, Y.; Yang, C.; Gao, F.; Zou, Y.; Li, Y. Tuning the Electron-Deficient Core of a Non-Fullerene Acceptor to Achieve over 17% Efficiency in a Single-Junction Organic Solar Cell. *Energy Environ. Sci.* **2020**, *13* (8), 2459–2466. https://doi.org/10.1039/D0EE00862A.

(34) Ye, L.; Weng, K.; Xu, J.; Du, X.; Chandrabose, S.; Chen, K.; Zhou, J.; Han, G.; Tan, S.; Xie, Z.; Yi, Y.; Li, N.; Liu, F.; Hodgkiss, J. M.; Brabec, C. J.; Sun, Y. Unraveling the Influence of Non-Fullerene Acceptor Molecular Packing on Photovoltaic Performance of Organic Solar Cells. *Nat. Commun.* **2020**, *11* (1), 6005. https://doi.org/10.1038/s41467-020-19853-z.

(35) Xu, Y.; Yao, H.; Ma, L.; Hong, L.; Li, J.; Liao, Q.; Zu, Y.; Wang, J.; Gao, M.; Ye, L.; Hou, J. Tuning the Hybridization of Local Exciton and Charge-Transfer States in Highly Efficient Organic Photovoltaic Cells. *Angew. Chemie* **2020**, *132* (23), 9089–9095. https://doi.org/10.1002/ange.201915030.

(36) Xie, Y.; Wang, W.; Huang, W.; Lin, F.; Li, T.; Liu, S.; Zhan, X.; Liang, Y.; Gao, C.; Wu, H.; Cao, Y. Assessing the Energy Offset at the Electron Donor/Acceptor Interface in Organic Solar Cells through Radiative Efficiency Measurements. *Energy Environ. Sci.* **2019**, *12* (12), 3556–3566. https://doi.org/10.1039/c9ee02939g.

(37) Zhang, M.; Zhu, L.; Zhou, G.; Hao, T.; Qiu, C.; Zhao, Z.; Hu, Q.; Larson, B. W.; Zhu, H.; Ma, Z.; Tang, Z.; Feng, W.; Zhang, Y.; Russell, T. P.; Liu, F. Single-Layered Organic Photovoltaics with Double Cascading Charge Transport Pathways: 18% Efficiencies. *Nat. Commun.* **2021**, *12* (1), 309. https://doi.org/10.1038/s41467-020-20580-8.

(38) Yang, D.; Wang, Y.; Sano, T.; Gao, F.; Sasabe, H.; Kido, J. A Minimal Non-Radiative Recombination Loss for Efficient Non-Fullerene All-Small-Molecule Organic Solar Cells with a Low Energy Loss of 0.54 EV and High Open-Circuit Voltage of 1.15 V. *J. Mater. Chem. A* **2018**, *6* (28), 13918–13924. https://doi.org/10.1039/c8ta04665d.

(39) Wang, Y.; Wang, Y.; Zhu, L.; Liu, H.; Fang, J.; Guo, X.; Liu, F.; Tang, Z.; Zhang, M.; Li, Y. A Novel Wide-Bandgap Small Molecule Donor for High Efficiency All-Small-Molecule Organic Solar Cells with Small Non-Radiative Energy Losses. *Energy Environ. Sci.* **2020**, *13* (5), 1309–1317. https://doi.org/10.1039/c9ee04199k.

(40) Xu, G.; Rao, H.; Liao, X.; Zhang, Y.; Wang, Y.; Xing, Z.; Hu, T.; Tan, L.; Chen, L.; Chen, Y. Reducing Energy Loss and Morphology Optimization Manipulated by Molecular Geometry Engineering for Hetero-Junction Organic Solar Cells. *Chinese J. Chem.* **2020**, *38* (12), 1553–1559. https://doi.org/10.1002/cjoc.202000235.

(41) Wu, J.; Fan, Q.; Xiong, M.; Wang, Q.; Chen, K.; Liu, H.; Gao, M.; Ye, L.; Guo, X.; Fang, J.; Guo, Q.; Su, W.; Ma, Z.; Tang, Z.; Wang, E.; Ade, H.; Zhang, M. Carboxylate Substituted Pyrazine: A Simple and Low-Cost Building Block for Novel Wide Bandgap Polymer Donor Enables 15.3% Efficiency in Organic Solar Cells. *Nano Energy* **2021**, *82*, 105679. https://doi.org/10.1016/j.nanoen.2020.105679.

(42) Sun, C.; Pan, F.; Chen, S.; Wang, R.; Sun, R.; Shang, Z.; Qiu, B.; Min, J.; Lv, M.; Meng, L.; Zhang, C.; Xiao, M.; Yang, C.; Li, Y. Achieving Fast Charge Separation and Low Nonradiative Recombination Loss by Rational Fluorination for High-Efficiency Polymer Solar Cells. *Adv. Mater.* **2019**, *31* (52), 1–8. https://doi.org/10.1002/adma.201905480.

(43) Li, X.; Weng, K.; Ryu, H. S.; Guo, J.; Zhang, X.; Xia, T.; Fu, H.; Wei, D.; Min, J.; Zhang, Y.; Woo, H. Y.; Sun, Y. Non-Fullerene Organic Solar Cells Based on Benzo[1,2-b:4,5-B']Difuran-Conjugated Polymer with 14% Efficiency. *Adv. Funct. Mater.* **2020**, *30* (6), 1–7. https://doi.org/10.1002/adfm.201906809.

(44) Gao, W.; Fu, H.; Li, Y.; Lin, F.; Sun, R.; Wu, Z.; Wu, X.; Zhong, C.; Min, J.; Luo, J.; Woo, H. Y.; Zhu, Z.; Jen, A. K. Y. Asymmetric Acceptors Enabling Organic Solar Cells to Achieve an over 17% Efficiency: Conformation Effects on Regulating Molecular Properties and Suppressing Nonradiative Energy Loss. *Adv. Energy Mater.* **2021**, *11* (4), 1–9. https://doi.org/10.1002/aenm.202003177.

(45) Sun, Y.; Gao, H.; Wu, S.; Meng, L.; Wan, X.; Li, M. Improving Current and Mitigating Energy Loss in Ternary Organic Photovoltaics Enabled by Two Well-Compatible Small Molecule Acceptors. **2021**, 1–8. https://doi.org/https://doi.org/10.1007/s11426-020-9921- 4 1.

(46) Pradhan, R.; Malhotra, P.; Gupta, G.; Singhal, R.; Sharma, G. D.; Mishra, A. Efficient Fullerene-Free Organic Solar Cells Using a Coumarin-Based Wide-Band-Gap Donor Material. *ACS Appl. Mater. Interfaces* **2020**, *12* (37), 41869–41876. https://doi.org/10.1021/acsami.0c12147.

(47) Tang, A.; Xiao, B.; Chen, F.; Zhang, J.; Wei, Z.; Zhou, E. The Introduction of Fluorine and Sulfur Atoms into Benzotriazole-Based p-Type Polymers to Match with a Benzotriazole-Containing n-Type Small Molecule: "The Same-Acceptor-Strategy" to Realize High Open-Circuit Voltage. *Adv. Energy Mater.* **2018**, *8* (25), 1–9. https://doi.org/10.1002/aenm.201801582.

(48) Chang, M.; Wang, Y.; Yi, Y. Q. Q.; Ke, X.; Wan, X.; Li, C.; Chen, Y. Fine-Tuning the Side-Chains of Non-Fullerene Small Molecule Acceptors to Match with Appropriate Polymer Donors. *J. Mater. Chem. A* **2018**, *6* (18), 8586–8594. https://doi.org/10.1039/c8ta00764k.

(49) Bin, H.; Zhang, Z. G.; Gao, L.; Chen, S.; Zhong, L.; Xue, L.; Yang, C.; Li, Y. Non-Fullerene Polymer Solar Cells Based on Alkylthio and Fluorine Substituted 2D-Conjugated Polymers Reach 9.5%

Efficiency. *J. Am. Chem. Soc.* **2016**, *138* (13), 4657–4664. https://doi.org/10.1021/jacs.6b01744.

(50) Huang, H.; Bin, H.; Peng, Z.; Qiu, B.; Sun, C.; Liebman-Pelaez, A.; Zhang, Z. G.; Zhu, C.; Ade, H.; Zhang, Z.; Li, Y. Effect of Side-Chain Engineering of Bithienylbenzodithiophene- Alt-Fluorobenzotriazole-Based Copolymers on the Thermal Stability and Photovoltaic Performance of Polymer Solar Cells. *Macromolecules* **2018**, *51* (15), 6028–6036. https://doi.org/10.1021/acs.macromol.8b01036.

(51) Zheng, Z.; Awartani, O. M.; Gautam, B.; Liu, D.; Qin, Y.; Li, W.; Bataller, A.; Gundogdu, K.; Ade, H.; Hou, J. Efficient Charge Transfer and Fine-Tuned Energy Level Alignment in a THF-Processed Fullerene-Free Organic Solar Cell with 11.3% Efficiency. *Adv. Mater.* **2017**, *29* (5), 1604241. https://doi.org/10.1002/adma.201604241.

(52) Luo, Z.; Li, G.; Gao, W.; Wu, K.; Zhang, Z. G.; Qiu, B.; Bin, H.; Xue, L.; Liu, F.; Li, Y.; Yang, C. A Universal Nonfullerene Electron Acceptor Matching with Different Band-Gap Polymer Donors for High-Performance Polymer Solar Cells. *J. Mater. Chem. A* **2018**, *6* (16), 6874–6881. https://doi.org/10.1039/c7ta11339k.

(53) Yang, F.; Li, C.; Lai, W.; Zhang, A.; Huang, H.; Li, W. Halogenated Conjugated Molecules for Ambipolar Field-Effect Transistors and Non-Fullerene Organic Solar Cells. *Mater. Chem. Front.* **2017**, *1* (7), 1389–1395. https://doi.org/10.1039/c7qm00025a.

(54) Dai, S.; Zhao, F.; Zhang, Q.; Lau, T. K.; Li, T.; Liu, K.; Ling, Q.; Wang, C.; Lu, X.; You, W.; Zhan, X. Fused Nonacyclic Electron Acceptors for Efficient Polymer Solar Cells. *J. Am. Chem. Soc.* **2017**, *139* (3), 1336–1343. https://doi.org/10.1021/jacs.6b12755.

(55) Hong, L.; Yao, H.; Yu, R.; Xu, Y.; Gao, B.; Ge, Z.; Hou, J. Investigating the Trade-Off between Device Performance and Energy Loss in Nonfullerene Organic Solar Cells. *ACS Appl. Mater. Interfaces* **2019**, *11* (32), 29124–29131. https://doi.org/10.1021/acsami.9b10243.

(56) Zhao, W.; Li, S.; Yao, H.; Zhang, S.; Zhang, Y.; Yang, B.; Hou, J. Molecular Optimization Enables over 13% Efficiency in Organic Solar Cells. *J. Am. Chem. Soc.* **2017**, *139* (21), 7148–7151. https://doi.org/10.1021/jacs.7b02677.

(57) Sun, H.; Sun, P.; Zhang, C.; Yang, Y.; Gao, X.; Chen, F.; Xu, Z.; Chen, Z. K.; Huang, W. High-Performance Organic Solar Cells Based on a Non-Fullerene Acceptor with a Spiro Core. *Chem. - An Asian J.* **2017**, *12* (7), 721–725. https://doi.org/10.1002/asia.201601741.

(58) Lin, H.; Chen, S.; Hu, H.; Zhang, L.; Ma, T.; Lai, J. Y. L.; Li, Z.; Qin, A.; Huang, X.; Tang, B.; Yan, H. Reduced Intramolecular Twisting Improves the Performance of 3D Molecular Acceptors in Non-Fullerene Organic Solar Cells. *Adv. Mater.* **2016**, *28* (38), 8546–8551. https://doi.org/10.1002/adma.201600997.

(59) Zhang, C. H.; Lin, F.; Huang, W.; Xin, J.; Wang, J.; Lin, Z.; Ma, W.; Yang, T.; Xia, J.; Liang, Y. Methyl Functionalization on Conjugated Side Chains for Polymer Solar Cells Processed from Non-Chlorinated Solvents. *J. Mater. Chem. C* **2020**, *8* (33), 11532–11539. https://doi.org/10.1039/d0tc02032j.

(60) Keshtov, M. L.; Kuklin, S. A.; Ostapov, I. E.; Makhaeva, E. E.; Suthar, R.; Dou, C.; Sharma, G. D. Acceptor Copolymers for Nonfullerene Polymer Solar Cells. **2020**, *2000611*, 1–9. https://doi.org/10.1002/ente.202000611.

(61) Li, C.; Zhou, J.; Song, J.; Xu, J.; Zhang, H.; Zhang, X.; Guo, J.; Zhu, L.; Wei, D.; Han, G.; Min, J.; Zhang, Y.; Xie, Z.; Yi, Y.; Yan, H.; Gao, F.; Liu, F.; Sun, Y. Non-Fullerene Acceptors with Branched Side Chains and Improved Molecular Packing to Exceed 18% Efficiency in Organic

Solar Cells. *Nat. Energy* **2021**, *6* (6), 605–613. https://doi.org/10.1038/s41560-021-00820-x.

(62) Song, X.; Gasparini, N.; Nahid, M. M.; Paleti, S. H. K.; Li, C.; Li, W.; Ade, H.; Baran, D. Efficient DPP Donor and Nonfullerene Acceptor Organic Solar Cells with High Photon-to-Current Ratio and Low Energetic Loss. *Adv. Funct. Mater.* **2019**, *1902441*, 1–8. https://doi.org/10.1002/adfm.201902441.

(63) Liu, Q.; Jiang, Y.; Jin, K.; Qin, J.; Xu, J.; Li, W.; Xiong, J.; Liu, J.; Xiao, Z.; Sun, K.; Yang, S.; Zhang, X.; Ding, L. 18% Efficiency Organic Solar Cells. *Sci. Bull.* **2020**, *65* (4), 272–275. https://doi.org/10.1016/j.scib.2020.01.001.

(64) Lin, Y.; Adilbekova, B.; Firdaus, Y.; Yengel, E.; Faber, H.; Sajjad, M.; Zheng, X.; Yarali, E.; Seitkhan, A.; Bakr, O. M.; El-Labban, A.; Schwingenschlögl, U.; Tung, V.; McCulloch, I.; Laquai, F.; Anthopoulos, T. D. 17% Efficient Organic Solar Cells Based on Liquid Exfoliated WS2 as a Replacement for PEDOT:PSS. *Adv. Mater.* **2019**, *31* (46). https://doi.org/10.1002/adma.201902965.

(65) Luo, Z.; Sun, C.; Chen, S.; Zhang, Z.-G.; Wu, K.; Qiu, B.; Yang, C.; Li, Y.; Yang, C. Side-Chain Impact on Molecular Orientation of Organic Semiconductor Acceptors: High Performance Nonfullerene Polymer Solar Cells with Thick Active Layer over 400 Nm. *Adv. Energy Mater.* **2018**, *8* (23), 1800856. https://doi.org/10.1002/aenm.201800856.

(66) Gao, L.; Zhang, Z. G.; Bin, H.; Xue, L.; Yang, Y.; Wang, C.; Liu, F.; Russell, T. P.; Li, Y. High-Efficiency Nonfullerene Polymer Solar Cells with Medium Bandgap Polymer Donor and Narrow Bandgap Organic Semiconductor Acceptor. *Adv. Mater.* **2016**, *28* (37), 8288–8295. https://doi.org/10.1002/adma.201601595.

(67) Li, M.; Liu, Y.; Ni, W.; Liu, F.; Feng, H.; Zhang, Y.; Liu, T.; Zhang, H.; Wan, X.; Kan, B.; Zhang, Q.; Russell, T. P.; Chen, Y. A Simple Small Molecule as an Acceptor for Fullerene-Free Organic Solar Cells with Efficiency near 8%. *J. Mater. Chem. A* **2016**, *4* (27), 10409–10413. https://doi.org/10.1039/c6ta04358e.

(68) Qiu, N.; Zhang, H.; Wan, X.; Li, C.; Ke, X.; Feng, H.; Kan, B.; Zhang, H.; Zhang, Q.; Lu, Y.; Chen, Y. A New Nonfullerene Electron Acceptor with a Ladder Type Backbone for High-Performance Organic Solar Cells. *Adv. Mater.* **2017**, *29* (6), 1–5. https://doi.org/10.1002/adma.201604964.

(69) Kan, B.; Feng, H.; Wan, X.; Liu, F.; Ke, X.; Wang, Y.; Wang, Y.; Zhang, H.; Li, C.; Hou, J.; Chen, Y. Small-Molecule Acceptor Based on the Heptacyclic Benzodi(Cyclopentadithiophene) Unit for Highly Efficient Nonfullerene Organic Solar Cells. *J. Am. Chem. Soc.* **2017**, *139* (13), 4929–4934. https://doi.org/10.1021/jacs.7b01170.

(70) Feng, H.; Qiu, N.; Wang, X.; Wang, Y.; Kan, B.; Wan, X.; Zhang, M.; Xia, A.; Li, C.; Liu, F.; Zhang, H.; Chen, Y. An A-D-A Type Small-Molecule Electron Acceptor with End-Extended Conjugation for High Performance Organic Solar Cells. *Chem. Mater.* **2017**, *29* (18), 7908–7917. https://doi.org/10.1021/acs.chemmater.7b02811.

(71) Li, R.; Liu, G.; Xiao, M.; Yang, X.; Liu, X.; Wang, Z.; Ying, L.; Huang, F.; Cao, Y. Non-Fullerene Acceptors Based on Fused-Ring Oligomers for Efficient Polymer Solar Cells: Via Complementary Light-Absorption. *J. Mater. Chem. A* **2017**, *5* (45), 23926–23936. https://doi.org/10.1039/c7ta06631g.

(72) Lin, Y.; Zhao, F.; Wu, Y.; Chen, K.; Xia, Y.; Li, G.; Prasad, S. K. K.; Zhu, J.; Huo, L.; Bin, H.; Zhang, Z. G.; Guo, X.; Zhang, M.; Sun, Y.; Gao, F.; Wei, Z.; Ma, W.; Wang, C.; Hodgkiss, J.; Bo, Z.; Inganäs, O.; Li, Y.; Zhan, X. Mapping Polymer Donors toward High-Efficiency Fullerene Free Organic Solar Cells. *Adv. Mater.* **2017**, *29* (3), 1–9. https://doi.org/10.1002/adma.201604155.

(73) Bin, H.; Yang, Y.; Peng, Z.; Ye, L.; Yao, J.; Zhong, L.; Sun, C.; Gao, L.; Huang, H.; Li, X.; Qiu, B.; Xue, L.; Zhang, Z. G.; Ade, H.; Li, Y. Effect of Alkylsilyl Side-Chain Structure on Photovoltaic Properties of Conjugated Polymer Donors. *Adv. Energy Mater.* **2018**, *8* (8), 1–8. https://doi.org/10.1002/aenm.201702324.

(74) Bin, H.; Zhong, L.; Yang, Y.; Gao, L.; Huang, H.; Sun, C.; Li, X.; Xue, L.; Zhang, Z. G.; Zhang, Z.; Li, Y. Medium Bandgap Polymer Donor Based on Bi(Trialkylsilylthienyl-Benzo[1,2-b:4,5-B″]-Difuran) for High Performance Nonfullerene Polymer Solar Cells. *Adv. Energy Mater.* **2017**, *7* (20), 1–7. https://doi.org/10.1002/aenm.201700746.

(75) Chen, T. W.; Peng, K. L.; Lin, Y. W.; Su, Y. J.; Ma, K. J.; Hong, L.; Chang, C. C.; Hou, J.; Hsu, C. S. A Chlorinated Nonacyclic Carbazole-Based Acceptor Affords over 15% Efficiency in Organic Solar Cells. *J. Mater. Chem. A* **2020**, *8* (3), 1131–1137. https://doi.org/10.1039/c9ta12605h.

(76) Miyake, Y.; Saeki, A. Machine Learning-Assisted Development of Organic Solar Cell Materials: Issues, Analyses, and Outlooks. *J. Phys. Chem. Lett.* **2021**, *12* (51), 12391–12401. https://doi.org/10.1021/acs.jpclett.1c03526.